

# Quantum speed limits based on Jensen-Shannon and Jeffreys divergences for general physical processes

Jucelino Ferreira de Sousa <sup>1</sup> and Diego Paiva Pires <sup>1,2</sup>

<sup>1</sup>*Programa de Pós-Graduação em Física, Universidade Federal do Maranhão, Campus Universitário do Bacanga, 65080-805, São Luís, Maranhão, Brazil*

<sup>2</sup>*Departamento de Física, Universidade Federal do Maranhão, Campus Universitário do Bacanga, 65080-805, São Luís, Maranhão, Brazil*

We discuss quantum speed limits (QSLs) for finite-dimensional quantum systems undergoing general physical processes. These QSLs were obtained using two families of entropic measures, namely the square root of the Jensen-Shannon divergence, which in turn defines a faithful distance of quantum states, and the square root of the quantum Jeffreys divergence. The results apply to both closed and open quantum systems, and are evaluated in terms of the Schatten speed of the evolved state, as well as cost functions that depend on the smallest and largest eigenvalues of both initial and instantaneous states of the quantum system. To illustrate our findings, we focus on the unitary and nonunitary dynamics of mixed single-qubit states. In the first case, we obtain speed limits *à la* Mandelstam-Tamm that are inversely proportional to the variance of the Hamiltonian driving the evolution. In the second case, we set the nonunitary dynamics to be described by the noisy operations: depolarizing channel, phase damping channel, and generalized amplitude damping channel. We provide analytical results for the two entropic measures, present numerical simulations to support our results on the speed limits, comment on the tightness of the bounds, and provide a comparison with previous QSLs. Our results may find applications in the study of quantum thermodynamics, entropic uncertainty relations, and also complexity of many-body systems.

## I. INTRODUCTION

Understanding entropic quantifiers has contributed to fundamental advances ranging from quantum information science to condensed matter physics [1]. On the one hand, entropic uncertainty relations paved the way for modern conceptual insights into Heisenberg's uncertainty principle [2, 3], also being useful in the characterization of quantum randomness [4], quantum key distribution [5], and scrambling of information [6]. On the other hand, entropic measures signal the role of entanglement in many-body quantum systems, also testifying criticality and phase transitions [7]. In addition, entropic measures have proven useful for characterizing quantum speed limits [8, 9].

Entropic measures also have a prominent role in the subject of quantum information processing, especially with regard to the task of distinguishing quantum states. The nonuniqueness of these quantifiers manifests itself in the existence of a zoo of entropies [10]. In this setting, quantum relative entropy (QRE) remains a paradigmatic entropic distinguishability measure of quantum states. QRE finds applications in a wide variety of physical scenarios, including the study of entanglement witnesses [11], quantum coherence measures [12], asymmetry of quantum states [13], and also entropy production [14]. Recent results address the interplay of the non-monotonic behavior of QRE and information backflow in quantum non-Markovian dynamics [15, 16].

Noteworthy, QRE has also been investigated within the scope of information geometry. It is a matter of fact that the Hessian matrix of QRE gives rise to the so-called Kubo-Mori inner product [17]. In this case, it is known that QRE plays a crucial role in the study of the geome-

try of work fluctuations in non-equilibrium quantum systems at finite temperature [18–20]. Furthermore, QRE provides a geometric understanding of the renormalisation group for finite-dimensional quantum systems [21]. However, QRE is an asymmetric distinguishability measure, and is therefore not a metric in the manifold of quantum states.

In this regard, suitable regularizations of QRE have been proposed to overcome this disadvantage, and a special role is played by the so-called quantum Jensen-Shannon divergence [22–24], and also the quantum Jeffreys divergence [25]. These quantifiers provide useful distinguishability measures of two probing quantum states, although they are not true distances, and are therefore called *divergences*. In fact, both measures are nonnegative, vanishing if and only if the input states are equal to each other, symmetric, but they do not satisfy the triangle inequality. These quantities find applications in the study of open quantum systems [26], graph symmetries and quantum walks [27], information processing [28], quantum coherence in multipartite systems [29], and also in the characterization of magic resource of quantum states and quantum gates for quantum computing [30].

QRE has also been applied in the study of quantum speed limits (QSLs), i.e., the minimum time required for the evolution of a given physical process. On the one hand, Ref. [31] addresses QSLs for closed quantum systems by means of Petz-Rényi and Tsallis relative entropies. On the other hand, Refs. [32, 33] analyzed speed limits for open quantum systems by using relative entropy of entanglement, and quantum mutual information. Recently, Ref. [34] studied a family of entropic QSLs based on  $\alpha$ - $z$ -Rényi relative entropies that apply to gene-

ral physical processes. To the best of our knowledge, despite numerous achievements regarding speed limits and relative entropies, understanding the interplay of QSLs, Jensen-Shannon divergence, and Jeffreys divergence, remains an issue to be addressed.

Here, we discuss the role of Jensen-Shannon and Jeffreys divergences in the characterization of quantum speed limits. To do so, we investigate the rate of change of these quantities and derive a class of speed limits for general physical processes. We specialize these results to the case of unitary dynamics and noisy quantum channels, thus showing that the bounds depend on the smallest and largest eigenvalues of the density matrix. Importantly, our results fit into the Mandelstam-Tamm class of speed limits. In particular, we set the case of initial single-qubit states, and evaluate the bounds for the depolarizing channel, phase damping channel, and generalized amplitude damping channel. We present numerical simulations to support our theoretical predictions.

The outline of the paper is as follows. In Sec. II, we review the main properties of entropic information-theoretic measures of quantum states. In Sec. III, we present upper bounds on the square roots of both Jensen-Shannon divergence and Jeffreys divergence for quantum states of a finite-dimensional quantum system undergoing a general physical process. In Sec. IV, we discuss quantum speed limits based on such entropic measures. In Secs. IV A and IV B, we investigate these entropic QSLs for the dynamics of closed and open quantum systems, respectively. We discuss the relation between these QSLs with results previously derived in literature, also addressing the tightness of both bounds. In Sec. V, we illustrate our findings for the unitary [see Sec. V A] and nonunitary [see Sec. V B] dynamics of single-qubit states. Finally, in Sec. VI we summarize our conclusions.

## II. ENTROPIC MEASURES

In this section, we briefly review the main properties of entropic information-theoretic quantifiers of quantum states. We consider a physical system described by finite-dimensional Hilbert space  $\mathcal{H}$ , with  $\dim(\mathcal{H}) = d$ . The state of the system is described by a density operator  $\rho \in \mathcal{S}$ , where  $\mathcal{S} = \{\rho \in \mathcal{H} \mid \rho^\dagger = \rho, \rho \geq 0, \text{Tr}(\rho) = 1\}$ . In this setting, given two density operators  $\rho, \varrho \in \mathcal{S}$ , the quantum relative entropy (QRE) is defined as [35, 36]

$$S(\rho\|\varrho) := \begin{cases} \text{Tr}[\rho(\ln \rho - \ln \varrho)] & \text{if } \text{supp}(\rho) \subseteq \text{supp}(\varrho), \\ +\infty & \text{otherwise,} \end{cases} \quad (1)$$

where  $\text{supp}(\bullet)$  is the support of the referred density matrix. We note that Eq. (1) was originally introduced by Umegaki over a half century ago [37, 38], and it stands for the quantum analogue of the classical Kullback-Leibler relative entropy [39]. In particular, the former recovers

the latter whenever the quantum states  $\rho$  and  $\varrho$  commute. We note that the QRE can be readily recast as  $S(\rho\|\varrho) = -S(\rho) - \text{Tr}(\rho \ln \varrho)$ , where  $S(\rho) = -\text{Tr}(\rho \ln \rho)$  is the von Neumann entropy.

Overall, QRE is (i) non-negative, i.e.,  $S(\rho\|\varrho) \geq 0$ , with  $S(\rho\|\varrho) = 0$  if and only if  $\rho = \varrho$ ; (ii) jointly convex, i.e.,  $\sum_l p_l S(\rho_l\|\varrho_l) \geq S(\sum_l p_l \rho_l\|\sum_l p_l \varrho_l)$ , with  $0 \leq p_l \leq 1$  and  $\sum_l p_l = 1$ ; (iii) isometric invariant,  $S(V\rho V^\dagger\|V\varrho V^\dagger) = S(\rho\|\varrho)$ , where  $V^\dagger = V^{-1}$  is a unitary operator; (iv) monotonically decreasing under completely positive and trace preserving (CPTP) maps, i.e.,  $S(\mathcal{E}(\rho)\|\mathcal{E}(\varrho)) \leq S(\rho\|\varrho)$ , with  $\mathcal{E}(\bullet)$  being a given CPTP operation; (v) additive,  $S(\rho_1 \otimes \rho_2\|\varrho_1 \otimes \varrho_2) = S(\rho_1\|\varrho_1) + S(\rho_2\|\varrho_2)$ , for all  $\{\rho_l, \varrho_l\}_{l=1,2} \in \mathcal{S}$ . For more details, see Refs. [1, 40] and references therein.

QRE satisfies several useful lower bounds and upper bounds. On the one hand, Pinsker inequality states that QRE is bounded from below by the trace distance, i.e.,  $S(\rho\|\varrho) \geq (1/2)\|\rho - \varrho\|_1^2$ , where  $\|A\|_1 = \text{Tr}(\sqrt{A^\dagger A})$  is the Schatten 1-norm [41]. On the other hand, QRE fulfills the upper bound  $S(\rho\|\varrho) \leq \|\rho - \varrho\|_2^2/\kappa_{\min}(\varrho)$ , with  $\|A\|_2 = \sqrt{\text{Tr}(A^\dagger A)}$  [42], while  $\kappa_{\min}(X)$  sets the smallest eigenvalue of the state  $X \in \mathcal{S}$ . In addition, QRE satisfies the chain of inequalities  $S_{\min}(\rho\|\varrho) \leq S(\rho\|\varrho) \leq S_{\max}(\rho\|\varrho)$ , where  $S_{\min}(\rho\|\varrho) = -\ln[\text{Tr}(\Pi_\rho \varrho)]$  sets the min-relative entropy, with  $\Pi_\rho$  being the projector onto  $\text{supp}(\rho)$ , while  $S_{\max}(\rho\|\varrho) = \ln[\min\{\lambda \mid \lambda \varrho - \rho \geq 0\}]$  defines the max-relative entropy, with  $\text{supp}(\rho) \subseteq \text{supp}(\varrho)$  [43].

It is worth noting that quantum relative entropy is an asymmetric distinguishability measure, i.e.,  $S(\rho\|\varrho) \neq S(\varrho\|\rho)$ , thus violating the triangular inequality. This means that QRE does not define a faithful metric over the space of quantum states. The asymmetry degree in QRE can be captured through the upper bound  $|S(\rho\|\varrho) - S(\varrho\|\rho)| \leq \mathcal{G}(\min(\kappa_{\min}(\rho), \kappa_{\min}(\varrho)), \|\rho - \varrho\|_1/2)$ , where  $\mathcal{G}(u, v) := g(u + v, u) - g(u, u + v)$  for all  $-1 \leq v \leq 1$  and  $\max(0, -v) \leq u \leq \min(1, 1 - v)$ , with  $g(p, q) := p \ln(p/q) + (1 - p) \ln[(1 - p)/(1 - q)]$  [44]. To the best of our knowledge, there are two ways to overcome the lack of symmetry, thus introducing symmetric information-theoretic quantities based on QRE.

On the one hand, the quantum Jeffreys divergence is defined as [25]

$$S_J(\rho\|\varrho) := \frac{1}{2}[S(\rho\|\varrho) + S(\varrho\|\rho)], \quad (2)$$

which is based on the *ad hoc* symmetrization of QRE. The subscript  $J$  refers to Jeffreys. Importantly, Eq. (2) defines the quantum analogue of the classical Jeffreys divergence, the latter being originally proposed about eighty years ago [45]. The factor 1/2 is included without loss of generality. It is worth mentioning that the classical Jeffreys divergence is not a metric on the space of probabilities, nor its square root [46, 47]. For our purposes, we consider the square root of the quantum

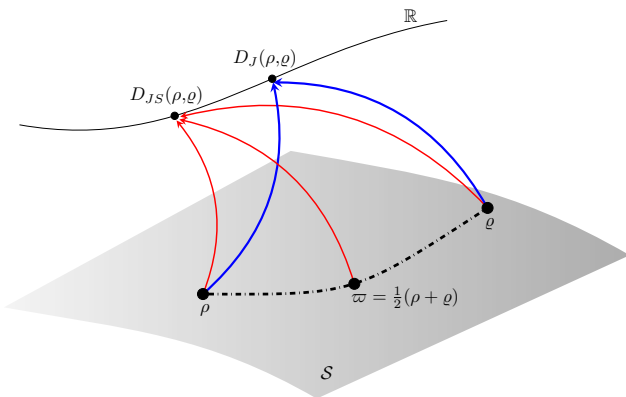


FIG. 1. (Color online) Overview of the role played by quantum Jeffreys pseudo-distance (QJPD),  $D_J(\rho, \varrho)$  [see Eq. (3)], and quantum Jensen-Shannon distance (QJSD),  $D_{JS}(\rho, \varrho)$  [see Eq. (6)]. QJPD (blue solid lines) and QJSD (solid red lines) map density matrices of the convex manifold of quantum states  $\mathcal{S}$  (gray smooth surface) to nonnegative numbers on the real line  $\mathbb{R}$  (black solid line), i.e.,  $D_{J,JS} : (\rho, \varrho) \in \mathcal{S} \mapsto \mathbb{R}$ . Noteworthy, QJSD takes into account the “average state”  $\varpi$ . QJSD is a faithful metric of quantum states, thus linking the distinguishability between  $\rho$  and  $\varrho$  to the length of a given path that connects these states (black dash-dotted line). QJPD, however, is not a true distance, but serves as a useful entropic measure.

Jeffreys divergence, which reads as

$$D_J(\rho, \varrho) := \sqrt{S_J(\rho||\varrho)} \\ = \sqrt{-\frac{1}{2}[S(\rho) + S(\varrho) + \text{Tr}(\rho \ln \varrho) + \text{Tr}(\varrho \ln \rho)]}. \quad (3)$$

Henceforth, we will refer to the distinguishability measure in Eq. (3) as the quantum Jeffreys pseudo-distance (QJPD). Noteworthy, QJPD is (i) non-negative,  $D_J(\rho, \varrho) \geq 0$ , with  $D_J(\rho, \varrho) = 0$  if and only if  $\rho = \varrho$ ; and (ii) symmetric,  $D_J(\rho, \varrho) = D_J(\varrho, \rho)$ , for all  $\rho, \varrho \in \mathcal{S}$ . So far, there is no proof that QJPD in Eq. (3) defines a faithful metric in the space of quantum states.

On the other hand, the quantum Jensen-Shannon divergence is defined as follows [22–24]

$$S_{JS}(\rho||\varrho) := \frac{1}{2}[S(\rho||\varpi) + S(\varrho||\varpi)], \quad (4)$$

where we introduce the convex combination

$$\varpi := \frac{1}{2}(\rho + \varrho). \quad (5)$$

To clarify, the subscript  $JS$  refers to Jensen-Shannon. Noteworthy, Eq. (4) stands as a distinguishability measure of quantum states that is based on a nontrivial symmetrization of the quantum relative entropy. It is bounded,  $0 \leq S_{JS}(\rho||\varrho) \leq 1$  for all  $\rho, \varrho \in \mathcal{S}$ , while for pure states  $\rho = |\psi\rangle\langle\psi|$  and  $\varrho = |\phi\rangle\langle\phi|$  it reduces to the von Neumann entropy of their convex combination, i.e.,  $S_{JS}(\rho||\varrho) = S(\varpi)$  [23]. Furthermore, it satisfies

the property  $S_{JS}(\rho_1 \otimes \rho_3 || \rho_2 \otimes \rho_3) = S_{JS}(\rho_1 || \rho_2)$ , for all  $\{\rho_l\}_{l=1,2,3} \in \mathcal{S}$  [22]. Quite recently, the square root of Jensen-Shannon divergence has been proved to define a *bona fide* metric over the space of quantum states [48]. This quantity can be written as

$$D_{JS}(\rho, \varrho) := \sqrt{S_{JS}(\rho||\varrho)} \\ = \sqrt{S(\varpi) - \frac{1}{2}[S(\rho) + S(\varrho)]}, \quad (6)$$

which will be called from now on the quantum Jensen-Shannon distance (QJSD). Importantly, QJSD is: (i) non-negative,  $D_{JS}(\rho, \varrho) \geq 0$ , with  $D_{JS}(\rho, \varrho) = 0$  if and only if  $\rho = \varrho$ ; (ii) symmetric,  $D_{JS}(\rho, \varrho) = D_{JS}(\varrho, \rho)$ ; (iii) and fulfills the triangular inequality,  $D_{JS}(\rho_1, \rho_3) \leq D_{JS}(\rho_1, \rho_2) + D_{JS}(\rho_2, \rho_3)$ , for all  $\{\rho_l\}_{l=1,2,3} \in \mathcal{S}$ . In Fig. 1, we show a schematic scenario of both QJPD and QJSD mappings.

### III. BOUNDING ENTROPIC MEASURES

In this section, we present upper bounds on the quantum Jeffreys pseudo-distance (QJPD) [see Sec. III A] and the quantum Jensen-Shannon distance (QJSD) [see Sec. III B] for quantum states of a physical system undergoing a general nonunitary dynamics. The system is initialized at the probe state  $\rho_0 \in \mathcal{S}$ , while  $\rho_t = \mathcal{E}_t(\rho_0)$  describes its respective evolved state when undergoing an arbitrary, time-dependent, nonunitary dynamics generated by the completely positive and trace preserving (CPTP) map  $\mathcal{E}_t(\bullet)$ , for all  $t \in [0, \tau]$ . Hereafter, we set  $\hbar = 1$ . By hypothesis, the instantaneous state  $\rho_t$  is described by a full-rank, nonsingular, and normal density matrix [49]. In this setting, it can be proved that QJPD and QJSD satisfy the upper bound

$$D_{J,JS}(\rho_0, \rho_\tau) \leq \sqrt{\int_0^\tau dt f_{J,JS}(\rho_0, \rho_t) \left\| \frac{d\rho_t}{dt} \right\|_1}, \quad (7)$$

where we introduce the cost function related to QJPD,

$$f_J(\rho_0, \rho_t) := \frac{1}{2} \left( |\ln(\kappa_{\min}(\rho_0) \kappa_{\min}(\rho_t))| + \frac{\kappa_{\max}(\rho_0)}{\kappa_{\min}(\rho_t)} \right), \quad (8)$$

and also the cost function related to QJSD

$$f_{JS}(\rho_0, \rho_t) := \frac{1}{2} \left| \ln \left( \kappa_{\min}(\rho_t) \kappa_{\min} \left( \frac{\rho_0 + \rho_t}{2} \right) \right) \right|, \quad (9)$$

while  $\kappa_{\min/\max}(\bullet)$  sets the smallest/largest eigenvalue of the referred density matrix, respectively. In the following, we provide details on the derivation of the bounds in Eq. (7), which are the first two main results of the paper. We also refer the reader to Appendices A, B, and C.

#### A. Bounding quantum Jeffreys pseudo-distance

We consider the QJPD,  $D_J(\rho_0, \rho_t)$ , as a symmetric distinguishability measure of the aforementioned quantum

states  $\rho_0$  and  $\rho_t$  [see Eq. (3)]. The absolute value of the time derivative of the squared QJPD satisfies the upper bound

$$\left| \frac{d}{dt} D_J^2(\rho_0, \rho_t) \right| \leq \frac{1}{2} \left| \frac{d}{dt} S(\rho_t) \right| + \frac{1}{2} \left| \text{Tr} \left( \rho_0 \frac{d}{dt} \ln \rho_t \right) \right| + \frac{1}{2} \left| \text{Tr} \left( \ln \rho_0 \frac{d\rho_t}{dt} \right) \right|, \quad (10)$$

where we have applied the triangle inequality, i.e.,  $|A_1 + A_2| \leq |A_1| + |A_2|$ . In Appendix B, we prove that the time derivative of von Neumann entropy becomes

$$\frac{d}{dt} S(\rho_t) = -\text{Tr} \left( \ln \rho_t \frac{d\rho_t}{dt} \right), \quad (11)$$

which holds for an arbitrary time-dependent density matrix  $\rho_t = \mathcal{E}_t(\rho_0) \in \mathcal{S}$  that undergoes a given physical process. In addition, in Appendix C we prove that

$$\left| \frac{d}{dt} \text{Tr}(\rho_0 \ln \rho_t) \right| \leq \frac{\kappa_{\max}(\rho_0)}{\kappa_{\min}(\rho_t)} \left\| \frac{d\rho_t}{dt} \right\|_1. \quad (12)$$

By combining Eqs. (10), (11), and (12), we conclude that the rate of change of the squared QJPD satisfies the upper bound

$$\left| \frac{d}{dt} D_J^2(\rho_0, \rho_t) \right| \leq f_J(\rho_0, \rho_t) \left\| \frac{d\rho_t}{dt} \right\|_1, \quad (13)$$

where the auxiliary function  $f_J(\rho_0, \rho_t)$  is defined in Eq. (8). We also use the fact that  $|\text{Tr}(A_1 A_2)| \leq \|A_1\|_\infty \|A_2\|_1$ , with  $\|\ln \bullet\|_\infty = |\ln(\kappa_{\min}(\bullet))|$ . To obtain an upper bound on QJPD, we integrate Eq. (13) over the time interval  $t \in [0, \tau]$ , thus obtaining the upper bound

$$D_J(\rho_0, \rho_\tau) \leq \sqrt{\int_0^\tau dt f_J(\rho_0, \rho_t) \left\| \frac{d\rho_t}{dt} \right\|_1}, \quad (14)$$

where we have applied the inequality  $|\int dt g(t)| \leq \int dt |g(t)|$ , and we also extract the square root of both sides of the resulting inequality. Equation (14) is the first result of the paper. We find that QJPD is bounded above by the square root of the time-averaged of Schatten speed  $\|d\rho_t/dt\|_1$ , weighted by the auxiliary function  $f_J(\rho_0, \rho_t)$ . The latter plays the role of a cost function that depends on the smallest/largest eigenvalues of both initial and instantaneous states of the system.

Based on Pinsker's inequality, it is known that quantum Jeffreys divergence satisfies the lower bound  $S_J(\rho_0 \| \rho_\tau) \geq (1/2) \|\rho_0 - \rho_\tau\|_1^2$ . In this case, from Eq. (14), one finds the chain of inequalities on QJPD as

$$\frac{\|\rho_0 - \rho_\tau\|_1}{\sqrt{2}} \leq D_J(\rho_0, \rho_\tau) \leq \sqrt{\int_0^\tau dt f_J(\rho_0, \rho_t) \left\| \frac{d\rho_t}{dt} \right\|_1}. \quad (15)$$

Overall, Eq. (15) provides a hierarchical bound on QJPD. On the one hand, QJPD is bounded from below by

the trace distance between initial and final states. On the other hand, QJPD is upper bounded by the time-averaged Schatten speed along the evolution path followed by the instantaneous quantum state.

## B. Bounding quantum Jensen-Shannon distance

Next, we present an upper bound on the square root of the QJSD, which in turn defines a metric on the space of quantum states. The absolute value of the time derivative of QJSD [see Eq. (6)] goes as follows

$$\left| \frac{d}{dt} D_{JS}^2(\rho_0, \rho_t) \right| \leq \left| \frac{d}{dt} S(\varpi_t) \right| + \frac{1}{2} \left| \frac{d}{dt} S(\rho_t) \right|, \quad (16)$$

where we have applied the triangular inequality,  $|A+B| \leq |A| + |B|$ , with  $\varpi_t := (1/2)(\rho_0 + \rho_t)$ . We note that  $\varpi_t \in \mathcal{S}$ , with  $\varpi_t^\dagger = \varpi_t$ ,  $\text{Tr}(\varpi_t) = 1$ , and  $\varpi_t \geq 0$ . From Eq. (11), one finds the rate of change  $dS(\varrho_t)/dt = -\text{Tr}[(d\varrho_t/dt) \ln \varrho_t]$  of the von Neumann entropy for an arbitrary time-dependent density matrix  $\varrho_t \in \mathcal{S}$  [see also Appendix B]. In this case, by using the matrix norm inequality  $|\text{Tr}(A_1 A_2)| \leq \|A_1\|_\infty \|A_2\|_1$ , we conclude that the rate of change of the von Neumann entropy satisfies the upper bound

$$\left| \frac{d}{dt} S(\varrho_t) \right| \leq \|\ln \varrho_t\|_\infty \left\| \frac{d\varrho_t}{dt} \right\|_1. \quad (17)$$

By combining Eqs. (16) and (17), we arrive at the result

$$\left| \frac{d}{dt} D_{JS}^2(\rho_0, \rho_t) \right| \leq \frac{1}{2} (\|\ln \varpi_t\|_\infty + \|\ln \rho_t\|_\infty) \left\| \frac{d\rho_t}{dt} \right\|_1. \quad (18)$$

Next, by integrating Eq. (18) over the time interval  $t \in [0, \tau]$ , one gets

$$D_{JS}(\rho_0, \rho_\tau) \leq \sqrt{\int_0^\tau dt f_{JS}(\rho_0, \rho_t) \left\| \frac{d\rho_t}{dt} \right\|_1}, \quad (19)$$

where we have used the inequality  $|\int dt g(t)| \leq \int dt |g(t)|$ , with  $|\ln(xy)| = |\ln x| + |\ln y|$  for all  $0 \leq x \leq 1$  and  $0 \leq y \leq 1$ , and we reinforce that the auxiliary function is defined in Eq. (9). Equation (19) is the second result of the paper. We note that QJSD is upper bounded by the square root of the Schatten speed weighted by the auxiliary function  $f_{JS}(\rho_0, \rho_t)$ , which in turn depends on the smallest eigenvalues of both instantaneous states  $\rho_t$  and  $\varpi_t$ .

## IV. QUANTUM SPEED LIMITS

The quantum speed limit (QSL) establishes a lower bound on the time of evolution of quantum systems [50, 51]. In the last decade, QSLs have found applications in the study of optimal control [52, 53], quantum batteries [54, 55], quantum correlations [56–59], quantum

computing [60, 61], quantum many-body systems [62–67], quantum thermodynamics [54, 68–70], non-Hermitian quantum systems [71–73]. We note that QSLs were also addressed in the subject of quantum-to-classical transitions [74–76]. Noteworthy, quantum speed limits have been investigated experimentally using trapped atoms [77], nuclear spins [78, 79], and also superconducting circuits [80]. QSLs were experimentally tested via a programmable superconducting quantum processor by emulating the dynamics of many-particle states [81].

The works of Mandelstam and Tamm (MT) [82] and Margolus and Levitin (ML) [83] represent a pivotal advance in the study of QSLs for closed quantum systems. These two results were unified by Levitin and Toffoli (LT) [84]. On the one hand, MT showed that the unitary evolution between two quantum states  $|\psi_0\rangle$  and  $|\psi_\tau\rangle$  implies the lower bound  $\tau \geq \tau_{MT}$ , where  $\tau_{MT} := (\hbar/\Delta E) \arccos(|\langle\psi_0|\psi_\tau\rangle|)$  is the minimum time of evolution between these states [82], and  $\Delta E = \sqrt{\langle H^2\rangle - \langle H\rangle^2}$  is the variance of a given time-independent Hamiltonian  $H$  that generates the dynamics. In particular, for orthogonal states such that  $\langle\psi_0|\psi_\tau\rangle = 0$ , the QSL time becomes  $\tau_{MT} = \pi\hbar/(2\Delta E)$ . On the other hand, ML proved that the minimum time of evolution for the unitary dynamics of two maximally distinguishable states satisfies the bound  $\tau \geq \tau_{ML}$ , with  $\tau_{ML} := \hbar\pi/[2(\langle\psi_0|H|\psi_0\rangle - E_0)]$  [83], where  $E_0$  is the lowest energy level of the system. In turn, LT proved a tighter QSL for orthogonal states by combining MT and ML bounds as  $\tau_{QSL} = \max\{\tau_{MT}, \tau_{ML}\}$  [84]. Recent advances involve the derivation of MT and ML bounds for pure and mixed states [85–87], correlated and separable states [88], as well as the discussion on the validity of the ML bound for time-dependent Hamiltonians [89–91]. It is noteworthy the study of QSLs for unitary dynamics exploring matrix norms [92, 93]. We highlight Ref. [94] which reported a speed limit that is dual to the ML bound, i.e., a QSL that depends on the highest energy level of the finite-dimensional quantum system.

Remarkable progress has been made in understanding QSLs in open quantum systems. Taddei *et al.* [95] presented an attainable QSL bound for that depends on the quantum Fisher information. In turn, del Campo *et al.* [96] derived a quantum speed limit from the relative purity of two quantum states of a given open quantum system. Notably, these last two results provide MT-like bounds for general physical processes. In contrast, Deffner and Lutz [97] obtained a ML-type bound written in terms of the operator norm of the generator of the nonunitary dynamics. It is worth noting that speed limits strongly depend on probe states and generators of the dynamical evolution [98–103]. QSLs have been obtained by exploiting geometric features of the quantum state space, mainly based on contractive Riemannian metrics [104–106] and Finsler geometry [107], thus providing tighter bounds. We also mention the derivation of speed limits for open quantum systems using Schatten  $p$ -norms [108–112].

Exploring the role of entropic distinguishability measures on the derivation of QSLs may be of interest in the study of entropic uncertainty relations [2, 3, 70]. In this scenario, paradigmatic figures of merit include von Neumann entropy, quantum relative entropy, Rényi entropies, to name a few. On the one hand, QSLs were addressed for closed quantum systems using Petz-Rényi and Tsallis relative entropies [31]. On the other hand, for open quantum systems, QSLs were investigated using negativity and quantum mutual information [32], relative entropy of entanglement [33], unified entropies [73], and most recently by means of  $\alpha$ - $z$ -Rényi relative entropies that apply to general physical processes [34]. Nonetheless, QSLs based on the Jensen-Shannon and Jeffreys divergences are still scarce in the literature, both for unitary or nonunitary dynamics. In the following, we derive a class of speed limits for general physical processes related to the quantum Jeffreys pseudo-distance [see Eq. (3)], and also based on the quantum Jensen-Shannon distance [see Eq. (6)].

We begin with the case of QJPD. Specifically, evaluating the time average of the right-hand side of Eq. (14), the time  $\tau$  required for an arbitrary nonunitary dynamics driving the state of the quantum system from  $\rho_0$  to  $\rho_\tau$  is lower bounded as  $\tau \geq \tau_J^{\text{QSL}}$ , with the QSL time related to QJPD given by

$$\tau_J^{\text{QSL}} := \frac{D_J^2(\rho_0, \rho_\tau)}{\langle\langle f_J(\rho_0, \rho_t) \| d\rho_t/dt \|_1 \rangle\rangle_\tau}, \quad (20)$$

where  $\langle\langle \bullet \rangle\rangle_\tau := (1/\tau) \int_0^\tau dt \bullet$  stands for the time average of a real-valued quantity. Equation (20) is the third result of the paper. In the following, we provide lower and upper bounds to the QSL time in Eq. (20). On the one hand, Pinsker's inequality applied to the initial  $\rho_0$  and final  $\rho_\tau$  states implies that the Jeffreys divergence is lower bounded by the squared Schatten 1-norm for these states, i.e.,  $S_J(\rho_0 \| \rho_\tau) \geq (1/2) \|\rho_0 - \rho_\tau\|_1^2$  [113]. In this case, one readily verifies that the QSL time in Eq. (20) is bounded from below as  $\tau_J^{\text{QSL}} \geq \tau_{J,\text{below}}^{\text{QSL}}$

$$\tau_{J,\text{below}}^{\text{QSL}} := \frac{\|\rho_0 - \rho_\tau\|_1^2}{2\langle\langle f_J(\rho_0, \rho_t) \| d\rho_t/dt \|_1 \rangle\rangle_\tau}, \quad (21)$$

where the trace distance signals how far apart the two states  $\rho_0$  and  $\rho_\tau$  are in the space of quantum states. On the other hand, since  $S(\rho_{0,\tau} \| \rho_{\tau,0}) \leq \|\rho_0 - \rho_\tau\|_2^2 / \kappa_{\min}(\rho_{\tau,0})$ , we conclude that the QSL time in Eq. (20) satisfies the upper bound  $\tau_J^{\text{QSL}} \leq \tau_{J,\text{above}}^{\text{QSL}}$

$$\tau_{J,\text{above}}^{\text{QSL}} := \frac{(\kappa_{\min}(\rho_0) + \kappa_{\min}(\rho_\tau)) \|\rho_0 - \rho_\tau\|_2^2}{2\langle\langle f_J(\rho_0, \rho_t) \| d\rho_t/dt \|_1 \rangle\rangle_\tau \kappa_{\min}(\rho_0) \kappa_{\min}(\rho_\tau)}, \quad (22)$$

which in turn depends on the Schatten 2-norm. It turns out that by combining Eqs. (21) and (22), the hierarchical bound  $\tau_{J,\text{below}}^{\text{QSL}} \leq \tau_J^{\text{QSL}} \leq \tau_{J,\text{above}}^{\text{QSL}}$  is found, which restricts the possible values of the QSL time based on QJPD.

Next, we address entropic speed limits based on QJSD, thus taking advantage from the bound in Eq. (19). The

time required for an arbitrary nonunitary dynamics driving the state of the quantum system from  $\rho_0$  to  $\rho_\tau$  is lower bounded as  $\tau \geq \tau_{JS}^{\text{QSL}}$ , where we define the entropic QSL time related to QJSD as follows

$$\tau_{JS}^{\text{QSL}} := \frac{D_{JS}^2(\rho_0, \rho_\tau)}{\langle\langle f_{JS}(\rho_0, \rho_t) \| d\rho_t/dt \|_1 \rangle\rangle_\tau}. \quad (23)$$

Equation (23) is the fourth result of the paper. The QSL time in Eq. (23) scales with the inverse of the time average of the Schatten speed, weighted by the cost function. It also depends on the quantum Jensen-Shannon distance that characterizes the distinguishability between the initial  $\rho_0$  and final  $\rho_\tau$  states. The bound requires a few quantities of the system, namely, the smallest eigenvalues of the initial and instantaneous states.

### A. QSLs and entropic measures in closed quantum systems

Here, we specialize the QSL bounds related to QJPD [see Eq. (20)], and also QJSD [see Eq. (23)] for the unitary dynamics of finite-dimensional closed quantum systems. We consider the dynamics of the closed system is governed by a time-independent Hamiltonian  $H$ , and the evolved state of the system is given by  $\rho_t = U_t \rho_0 U_t^\dagger$ , with  $U_t = e^{-itH}$  being the evolution operator. In this case, the Schatten speed reads as  $\|d\rho_t/dt\|_1 = \|(-i)[H, \rho_0]\|_1$ .

For the QJPD, the speed limit time in Eq. (20) becomes

$$\tau_J^{\text{QSL}} = \frac{D_J^2(\rho_0, \rho_\tau)}{(|\ln(\kappa_{\min}(\rho_0))| + \eta(\rho_0)/2) \|(-i)[H, \rho_0]\|_1}, \quad (24)$$

where  $\eta(\rho_0) := \kappa_{\max}(\rho_0)/\kappa_{\min}(\rho_0)$  stands for the condition number of the density matrix [114]. It is worth noting that the eigenvalues of the density matrix remain unchanged under unitary evolutions, i.e.,  $\kappa_{\min/\max}(\rho_t) = \kappa_{\min/\max}(\rho_0)$ , for all  $0 \leq t \leq \tau$ . For the QJSD, the QSL bound in Eq. (23) yields

$$\tau_{JS}^{\text{QSL}} := \frac{2D_{JS}^2(\rho_0, \rho_\tau)}{\langle\langle |\ln(\kappa_{\min}(\rho_0) \kappa_{\min}(\frac{\rho_0 + \rho_t}{2}))| \rangle\rangle_\tau \|(-i)[H, \rho_0]\|_1}, \quad (25)$$

where we have used the fact that the convex sum  $\varpi_t = (1/2)(\rho_0 + \rho_t)$  exhibits time-dependent eigenvalues, since  $\rho_0$  and  $\rho_t$  are noncommuting density matrices.

Equations (25) and (24) represent the fifth result of the paper. They fit into the class of Mandelstam-Tamm speed limits. To see this point, we note that  $\|(-i)[H, \rho_0]\|_1 \leq 2\Delta H$ , where  $(\Delta H)^2 = \text{Tr}(\rho_0 H^2) - [\text{Tr}(\rho_0 H)]^2$  is the variance of the Hamiltonian  $H$  [115–118]. Hence, we have that the entropic QSLs are bounded from below as  $\tau_J^{\text{QSL}} \geq D_J^2(\rho_0, \rho_\tau)/[(2|\ln(\kappa_{\min}(\rho_0))| + \eta(\rho_0))\Delta H]$ , and  $\tau_{JS}^{\text{QSL}} \geq D_{JS}^2(\rho_0, \rho_\tau)/[\langle\langle |\ln(\kappa_{\min}(\rho_0) \kappa_{\min}(\frac{\rho_0 + \rho_t}{2}))| \rangle\rangle_\tau \Delta H]$ , both of them related to the fluctuations of the generator of the dynamics.

It is worth noting that Ref. [31] reported a speed limit for closed quantum systems using symmetrized relative entropy. In detail, such a bound was obtained via Cauchy-Schwarz inequality, and depends on the Schatten 2-norm of the commutator of the Hamiltonian and the probe/evolved state of the system, and also the Schatten 2-norm of the logarithm of the initial state. However, Eq. (24) is expected to be tighter since it was derived via Hölder's inequality related to Schatten 1-norm and operator norm. In addition to the squared QJPD, i.e., the symmetrized relative entropy, Eq. (24) depends on the smallest/largest eigenvalues of the probe state, and also on the Schatten 1-norm of the commutator of the Hamiltonian and the initial state of the system.

### B. QSLs and entropic measures in open quantum systems

Here, we illustrate the results in Eqs. (20) and (23) for the nonunitary dynamics governed by the completely positive and trace-preserving (CPTP) map,  $\mathcal{E}_t(\bullet) = \sum_j K_j \bullet K_j^\dagger$ , with  $\{K_j\}_{j=1, \dots, s}$  being the set of time-dependent Kraus operators, with  $\sum_j K_j^\dagger K_j = \mathbb{I}$  [35]. In this framework, by applying the triangular inequality  $\|\sum_j \mathcal{O}_j\|_1 \leq \sum_j \|\mathcal{O}_j\|_1$ , and also using the invariance of the Schatten norm  $\|\mathcal{O}^\dagger\|_1 = \|\mathcal{O}\|_1$ , one obtains the upper bound on the Schatten speed as  $\|d\rho_t/dt\|_1 \leq 2\sum_j \|K_j \rho_0 (dK_j^\dagger/dt)\|_1$ . Therefore, by substituting this result in Eqs. (20) and (23), one gets the QSL time based on QJPD as

$$\tau_J^{\text{QSL}} = \frac{D_J^2(\rho_0, \rho_\tau)}{2 \langle\langle f_J(\rho_0, \rho_t) \sum_j \|K_j \rho_0 (dK_j^\dagger/dt)\|_1 \rangle\rangle_\tau}, \quad (26)$$

and also the QSL time based on QJSD as

$$\tau_{JS}^{\text{QSL}} = \frac{D_{JS}^2(\rho_0, \rho_\tau)}{2 \langle\langle f_{JS}(\rho_0, \rho_t) \sum_j \|K_j \rho_0 (dK_j^\dagger/dt)\|_1 \rangle\rangle_\tau}, \quad (27)$$

with the cost functions  $f_{J, JS}(\rho_0, \rho_t)$  given in Eqs. (8) and (9), respectively.

The entropic QSL bounds in Eqs. (26) and (27) describe the sixth result of the paper. They are characterized by the smallest/largest eigenvalues of probe and evolved states that are encoded in each of the cost functions, and also by the set of Kraus operators that describes the effective nonunitary dynamics of the finite-dimensional quantum system. Furthermore, it turns out that  $\tau_J^{\text{QSL}}$  and  $\tau_{JS}^{\text{QSL}}$  depend on QJPD and QJSD, respectively, both entropic quantities capturing the distinguishability between initial  $\rho_0$  and final  $\rho_\tau$  states of the dynamics.

In the following, we compare Eqs. (26) and (27) with previous QSLs addressed in the literature. On the one hand, Refs. [9, 32, 33] discussed speed limits based on relative entropies of entanglement that depend on prior

knowledge of the full spectrum of the Liouvillians that governs the nonunitary dynamics. On the other hand, Ref. [73] presents QSLs based on unified entropies for general physical processes. This family of entropies does not encompass QJPD nor QJSD as particular cases. Next, Ref. [34] reported entropic QSLs based on  $\alpha$ - $z$ -Rényi relative entropies, the latter recovering Umegaki's relative entropy by fixing  $z = 1$  and taking  $\alpha \rightarrow 1$ . However, we note that such speed limits are valid only for  $\alpha \in (0, 1)$  and  $\max\{\alpha, 1 - \alpha\} \leq z \leq 1$ , which implies that they can not provide QSLs related to standard quantum relative entropy. Last but not least, since a different combination of inequalities was used to derive Eqs. (26) and (27), one expects that another type of speed limit would be obtained when compared to the results in Ref. [34].

## V. EXAMPLES

To illustrate our findings, we consider a two-level system initialized at the mixed single-qubit state  $\rho_0 = (1/2)(\mathbb{I} + \vec{r} \cdot \vec{\sigma})$ , where  $\vec{r} = r\hat{r}$  is the Bloch vector, with  $\hat{r} = (\sin\theta \cos\phi, \sin\theta \sin\phi, \cos\theta)$ , where  $0 \leq r < 1$ ,  $0 \leq \theta \leq \pi$ , and  $0 \leq \phi < 2\pi$ , while  $\vec{\sigma} = (\sigma_x, \sigma_y, \sigma_z)$  is the vector of Pauli matrices, and  $\mathbb{I}$  is the  $2 \times 2$  identity matrix. The initial state exhibits the eigenvalues  $\kappa_{\max/\min}(\rho_0) = (1/2)(1 \pm r)$ . On the one hand, we investigate the entropic QSLs for unitary evolutions generated by time-independent Hamiltonians [see Sec. V A]. On the other hand, we address the QSLs related to nonunitary evolutions of single-qubit states in terms of some prototypical quantum channels [see Sec. V B].

### A. Unitary evolution

Let  $H = \vec{n} \cdot \vec{\sigma}$  be a time-independent Hamiltonian driving the unitary evolution of the prototype two-level system, where  $\vec{n} = (n_x, n_y, n_z)$  is a three-dimensional vector. We note that  $\|(-i)[H, \rho_0]\|_1 = 2r\|\vec{n}\|\|\hat{n} \times \hat{r}\|$ , where  $\hat{n} = \vec{n}/\|\vec{n}\|$  is a unit vector, with  $\|\vec{n}\|^2 = n_x^2 + n_y^2 + n_z^2$  being the squared Euclidean norm. The instantaneous state of the system is given by  $\rho_t^C = U_t \rho_0 U_t^\dagger = (1/2)(\mathbb{I} + \vec{r}_t \cdot \vec{\sigma})$ , where  $U_t = e^{-itH} = \cos(\|\vec{n}\|t)\mathbb{I} - i \sin(\|\vec{n}\|t)(\hat{n} \cdot \vec{\sigma})$  is the unitary evolution operator, with  $U_t U_t^\dagger = U_t^\dagger U_t = \mathbb{I}$ . In turn, the convex combination  $\varpi_t^C = (1/2)(\rho_0 + \rho_t^C) = (1/2)(\mathbb{I} + (1/2)(\vec{r} + \vec{r}_t) \cdot \vec{\sigma})$  displays the eigenvalues  $\kappa_{\max/\min}(\varpi_t^C) = (1/2)(1 \pm \nu_t^C)$ , where we define

$$\nu_t^C := r \sqrt{1 - \|\hat{n} \times \hat{r}\|^2 \sin^2(\|\vec{n}\|t)}. \quad (28)$$

Next, we address the entropic QSL time based on QJPD [see Eq. (24)]. To do so, we first evaluate QJPD, thus finding that  $D_J(\rho_0, \rho_\tau^C) = \sqrt{S(\rho_0 \| \rho_\tau^C)}$ , where the Umegaki relative entropy for single-qubit states is given

by [see Appendix D]

$$S(\rho_0 \| \rho_\tau^C) = r \ln \left( \frac{1+r}{1-r} \right) \|\hat{n} \times \hat{r}\|^2 \sin^2(\|\vec{n}\|\tau). \quad (29)$$

Hence, the time required for a unitary process driving the state of the quantum system from  $\rho_0$  to  $\rho_\tau$  is lower bounded as  $\tau \geq \tau_J^{\text{QSL}}$ , where

$$\tau_J^{\text{QSL}} = \frac{\|\hat{n} \times \hat{r}\| \ln \left( \frac{1+r}{1-r} \right) \sin^2(\|\vec{n}\|\tau)}{\|\vec{n}\| \left( 2 \left| \ln \left( \frac{1-r}{2} \right) \right| + \frac{1+r}{1-r} \right)}. \quad (30)$$

It is worth noting that  $\tau_J^{\text{QSL}}$  in Eq. (30) is a harmonic function of the dimensionless parameter  $\|\vec{n}\|\tau$ , thus going to zero for all  $\|\vec{n}\|\tau = k\pi$ , with  $k \in \mathbb{N}$ . In particular, for  $\|\vec{n}\|\tau \ll 1$ , it approaches the value  $\tau_J^{\text{QSL}} \approx \|\hat{n} \times \hat{r}\| \|\vec{n}\| \tau^2 \ln[(1+r)/(1-r)] / (2 |\ln[(1-r)/2]| + (1+r)/(1-r))$ , and grows quadratically with time  $\tau$ . The entropic QSL time in Eq. (30) is sensitive to the role played by the coherences of the probe state with respect to the energy eigenstates of the Hamiltonian. To see this point, one verifies that  $\|\hat{n} \times \hat{r}\| = \sqrt{1 - (\hat{n} \cdot \hat{r})^2} = \sqrt{2 \mathcal{I}_H(\rho_0) / (\|\vec{n}\|r)}$ , where  $\mathcal{I}_H(\rho_0) = -(1/4)\text{Tr}[(\rho_0, H)^2]$  is a coherence measure [119]. This means that the minimum time it takes to change the state of the system will be influenced by the amount of coherences stored in its initial state. We find that  $\tau_J^{\text{QSL}}$  in Eq. (30) vanishes for probe states that are incoherent with respect to the eigenbasis of  $H$ , i.e., one gets  $\tau_J^{\text{QSL}} = 0$  for parallel unit vectors  $\hat{r}$  and  $\hat{n}$ .

To conclude, we investigate the QSL time based on the QJSD metric. In detail, we find that  $D_{JS}(\rho_0, \rho_\tau^C) = \sqrt{S(\varpi_\tau^C) - S(\rho_0)}$ , which comes from the fact the von Neumann entropy remains invariant for input states undergoing unitary evolutions, i.e.,  $S(U_t \rho_0 U_t^\dagger) = S(\rho_0)$  for all  $t > 0$ . In this case, Eq. (25) becomes

$$\tau_{JS}^{\text{QSL}} := \frac{h(\frac{1-r}{2}) - h(\frac{1-\nu_\tau^C}{2})}{r \|\vec{n}\| \|\hat{n} \times \hat{r}\| \left\langle \left\langle \left| \ln \left( \frac{(1-r)(1-\nu_\tau^C)}{4} \right) \right| \right\rangle \right\rangle_\tau}, \quad (31)$$

where we define

$$h(x) := x \ln x + (1-x) \ln(1-x), \quad (32)$$

with  $0 \leq x \leq 1$ . We note that Eq. (31) is fully characterized by the parameters  $r$ ,  $\|\vec{n}\|$ , and  $\tau$ , also depending on the Euclidean norm  $\|\hat{n} \times \hat{r}\|$  that displays the role of the coherences of the probe state  $\rho_0$  with respect to the eigenstates of the Hamiltonian  $H$ . On the one hand, for  $\|\vec{n}\|\tau \ll 1$ , Eq. (31) approaches the value  $\tau_{JS}^{\text{QSL}} \approx \|\hat{n} \times \hat{r}\| \ln[(1-r)/(1+r)] \|\vec{n}\| \tau^2 / (8 \ln[(1-r)/2])$  at earlier times of the dynamics. On the other hand, for all  $t > 0$ , using the L'Hospital rule, we note that  $\lim_{\|\hat{n} \times \hat{r}\| \rightarrow 0} \tau_{JS}^{\text{QSL}} = 0$ , i.e., the entropic QSL time is zero-valued for initial incoherent states such that  $\|\hat{n} \times \hat{r}\| = 0$ , as expected. In particular, for  $0 < \|\hat{n} \times \hat{r}\| \ll 1$  and  $t > 0$ , it can be verified that the lowest approximation order of Eq. (31) with respect to such a quantity is given by  $\tau_{JS}^{\text{QSL}} \approx \|\hat{n} \times \hat{r}\| \ln[(1-r)/(1+r)] \sin^2(\|\vec{n}\|\tau) / (8 \|\vec{n}\| \ln[(1-r)/2])$ .

TABLE I. Information-theoretic quantities related to the entropic QSLs for single-qubit states evolving under the quantum channels depolarizing, phase damping, and generalized amplitude damping channel. Here,  $\lambda_t = 1 - e^{-\Gamma t}$ , with  $\Gamma$  being the decoherence rate. We also define  $c_{s\alpha} = (1/2)(1 + (-1)^s) + (-1)^{s-1}\alpha$ , with  $s = \{1, 2\}$ , where  $\alpha \in [0, 1]$  is a dimensionless parameter that encodes the temperature effects in the noisy channel.

Quantum channel	Useful quantity	Analytical value
Depolarizing (Sec. VB 1)	$r_t^D$	$(1 - \lambda_t)r$
	$\nu_t^D$	$(1 - \frac{\lambda_t}{2})r$
	$\sum_{l=0}^3 \ K_l \rho_0 (dK_l^\dagger / dt)\ _1$	$\frac{3\Gamma}{4}(1 - \lambda_t)$
Phase damping (Sec. VB 2)	$r_t^{PD}$	$r\sqrt{1 - \lambda_t \sin^2 \theta}$
	$\nu_t^{PD}$	$r\sqrt{1 - \frac{1}{4}(\lambda_t + 2(1 - \sqrt{1 - \lambda_t})) \sin^2 \theta}$
	$\sum_{l=0}^1 \ K_l \rho_0 (dK_l^\dagger / dt)\ _1$	$\frac{\Gamma}{4}(1 - \lambda_t) \left(1 - r \cos \theta + \sqrt{(1 - r \cos \theta)^2 + \frac{r^2 \sin^2 \theta}{1 - \lambda_t}}\right)$
Generalized amplitude damping (Sec. VB 3)	$r_t^{GAD}$	$\sqrt{[(2\alpha - 1)\lambda_t + (1 - \lambda_t)r \cos \theta]^2 + (1 - \lambda_t)r^2 \sin^2 \theta}$
	$\nu_t^{GAD}$	$\frac{1}{2} \left\{ \lambda_t(2\alpha - 1)(2(2 - \lambda_t)r \cos \theta + \lambda_t(2\alpha - 1)) + r^2 [(2 - \lambda_t)^2 + (2 - (2 - \lambda_t)\sqrt{1 - \lambda_t})\sqrt{1 - \lambda_t} \sin^2 \theta] \right\}^{1/2}$
	$\sum_{l=0}^3 \ K_l \rho_0 (dK_l^\dagger / dt)\ _1$	$\frac{\Gamma(1 - \lambda_t)}{4} \sum_{s=1}^2 c_{s\alpha} \left(1 + (-1)^s r \cos \theta + \sqrt{(1 + (-1)^s r \cos \theta)^2 + \frac{r^2 \sin^2 \theta}{1 - \lambda_t}}\right)$

## B. Nonunitary evolution

In the following, we address the QSLs related to nonunitary evolutions described by the quantum noisy operations: (i) depolarizing channel [see Sec. VB 1], (ii) phase damping channel [see Sec. VB 2], and (iii) generalized amplitude damping channel (GAD) [see Sec. VB 3]. The study of these QSLs takes into account Eqs. (26) and (27). Throughout the text, we report analytical expressions for QJPD, QJSD and other quantities useful for calculating such entropic QSLs for each of the quantum channels considered. In Table I, we summarize the results and provide some additional data.

To investigate the tightness of the QSLs, we consider the figure of merit defined as follows

$$\delta_{J,JS}(\tau) := 1 - \frac{\tau_{J,JS}^{\text{QSL}}}{\tau}. \quad (33)$$

In Eq. (33), the smaller the relative error, the tighter the entropic speed limit related to QJSD and QJPD. The figure of merit signals the deviation of the QSL bound concerning the average quantum speed. The bounds saturate whenever  $D_{J,JS}^2(\rho_0, \rho_\tau)$  coincides with the time-average of the product between the cost function  $f_{J,JS}(\rho_0, \rho_t)$  and the Schatten speed that is induced by the overall dynamics. For convenience, throughout the paper we will focus on the normalized relative error  $\tilde{\delta}_{J,JS}(\tau)$ , with  $\tilde{x} := (x - \min(x))/(\max(x) - \min(x))$ , observing that  $0 \leq \tilde{\delta}_{J,JS}(\tau) \leq 1$ .

### 1. Depolarizing channel

The depolarizing channel is described by the Kraus operators  $K_0 = \sqrt{1 - (3\lambda_t/4)} \mathbb{I}$ , and  $K_{1,2,3} = \sqrt{\lambda_t/4} \sigma_{x,y,z}$ , with  $\lambda_t = 1 - e^{-\Gamma t}$ , where  $\Gamma$  is the damping constant [35]. We note that this quantum channel is unital, i.e.,  $\sum_{l=0}^3 K_l^\dagger K_l = \sum_{l=0}^3 K_l K_l^\dagger = \mathbb{I}$ . The evolved state of the two-level system becomes  $\rho_t^D = \sum_{l=0}^3 K_l \rho_0 K_l^\dagger = (1/2)(\mathbb{I} + r_t^D(\hat{r} \cdot \vec{\sigma}))$ , where we define  $r_t^D = (1 - \lambda_t)r$ . This state has eigenvalues  $\kappa_{\max/\min}(\rho_t^D) = (1 \pm r_t^D)/2$ . We recall that the quantum channel uniformly shrinks the Bloch sphere towards its center, thus fully depolarizing the initial single-qubit state. In fact, for  $\Gamma t \gg 1$ , the stationary state  $\rho_\infty^D \approx \mathbb{I}/2$  is the maximally mixed one. In turn, one finds the state  $\varpi_t^D = (\rho_0 + \rho_t^D)/2 = (1/2)(\mathbb{I} + \nu_t^D(\hat{r} \cdot \vec{\sigma}))$ , where  $\nu_t^D = (1 - \lambda_t/2)r$ , with eigenvalues  $\kappa_{\max/\min}(\varpi_t^D) = (1/2)(1 \pm \nu_t^D)$ .

In this setting, one finds that the quantum Jeffreys pseudo-divergence related to initial  $\rho_0$  and evolved  $\rho_\tau^D$  states yields

$$D_J(\rho_0, \rho_\tau^D) = \frac{1}{2} \sqrt{(r - r_\tau^D) \ln \left[ \frac{(1+r)(1-r_\tau^D)}{(1-r)(1+r_\tau^D)} \right]}. \quad (34)$$

Equation (34) shows that QJPD is independent of the parameters  $\theta$  and  $\phi$ , being function of the dimensionless parameters  $\Gamma\tau$  and  $r$ . On the one hand, for  $\Gamma\tau \ll 1$ , QJPD becomes  $D_J^2(\rho_0, \rho_\tau^D) \approx (r^2/2)(\Gamma\tau)^2/(1 - r^2)$ . On the other hand, for  $\Gamma\tau \gg 1$ , QJPD approaches the asymptotic value  $D_J^2(\rho_0, \rho_\tau^D) \approx (r/4) \ln[(1+r)/(1-r)]$ , being

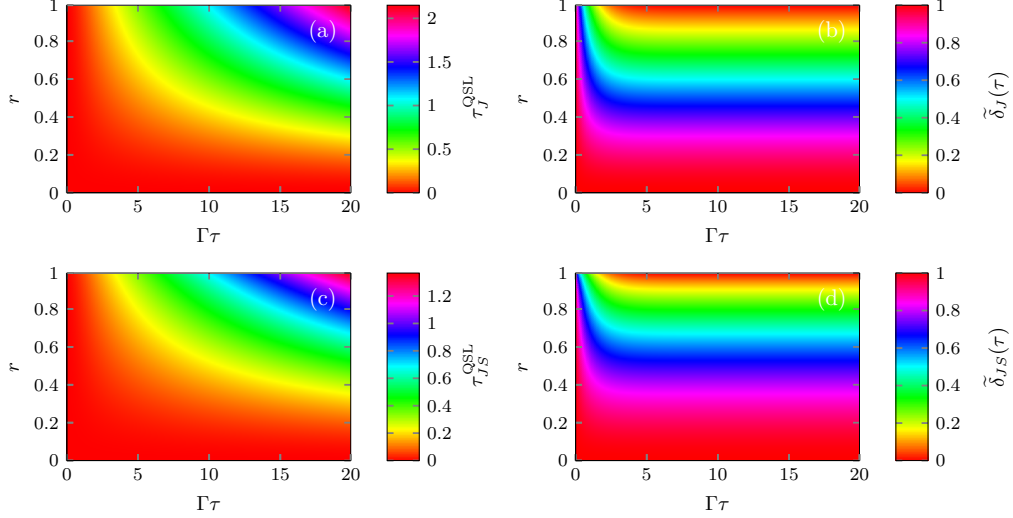


FIG. 2. (Color online) Density plot of the entropic QSLs  $\tau_{J,J_S}^{\text{QSL}}$  [see Eqs. (35) and (37), respectively], and the normalized relative errors  $\tilde{\delta}_{J,J_S}(\tau)$  [see Eq. (33)], as a function of the dimensionless parameters  $\Gamma\tau$  and  $r \in [0, 1)$ , for initial single-qubit states evolving under the depolarizing channel [see Sec. VB 1]. Here, we consider  $\theta \in [0, \pi]$  and  $\phi \in [0, 2\pi)$ .

fully characterized by the mixedness parameter  $r \in [0, 1)$ . The latter result is in agreement with the fact that the system approaches the maximally mixed state  $\mathbb{I}/2$  for  $\Gamma\tau \gg 1$ .

Next, the QSL time based on QJPD is evaluated as follows

$$\begin{aligned} \frac{\tau_J^{\text{QSL}}}{\tau} &= \frac{r}{3}(1 - e^{-\Gamma\tau}) \left[ \ln\left(\frac{1+r}{1-r}\right) - \ln\left(\frac{1+r_\tau^D}{1-r_\tau^D}\right) \right] \\ &\times \left[ (1 + e^{-\Gamma\tau}) \ln(1 - re^{-\Gamma\tau}) - (3 - e^{-\Gamma\tau}) \ln(1 - r) \right. \\ &\left. + (1 - e^{-\Gamma\tau})(2 \ln 2 + 1) \right]^{-1}. \end{aligned} \quad (35)$$

On the one hand, for  $\Gamma\tau \ll 1$ , we verify that  $\tau_J^{\text{QSL}}/\tau \approx 2r^2\Gamma\tau/\{3(1+r)[1+r+(1-r)(\ln 4 - 2\ln(1-r))]\}$ , thus increasing linearly with  $\Gamma\tau$  at earlier times of the dynamics. On the other hand, for  $\Gamma\tau \gg 1$ , one obtains the ratio  $\tau_J^{\text{QSL}}/\tau \approx (r/3) \ln[(1+r)/(1-r)]/[2 \ln 2 + 1 - 3 \ln(1-r)]$ , thus being a time-independent quantity at later times of the dynamics.

In turn, the quantum Jensen-Shannon distance can be written as

$$\begin{aligned} D_{JS}(\rho_0, \rho_\tau^D) &= \\ &\frac{1}{\sqrt{2}} \sqrt{h\left(\frac{1-r}{2}\right) + h\left(\frac{1-r_\tau^D}{2}\right) - 2h\left(\frac{1-r_\tau^D}{2}\right)}, \end{aligned} \quad (36)$$

with  $h(\bullet)$  defined in Eq. (32). It is worth noting that QJSD is a function of  $r$  and  $\Gamma\tau$ . In this case, the mixedness degree of the initial state  $\rho_0$  strongly accounts for its distinguishability from any instantaneous single-qubit state. In particular, for  $\Gamma\tau \ll 1$ , one finds that the squared QJSD becomes  $D_{JS}^2(\rho_0, \rho_\tau^D) \approx (r^2/8)(\Gamma\tau)^2/(1-r^2)$ , thus increasing quadratically with

the dimensionless parameter  $\Gamma\tau$ . However, for  $\Gamma\tau \gg 1$ , the squared QJSD approaches the asymptotic, time-independent value  $D_{JS}^2(\rho_0, \rho_\tau^D) \approx (1/2)[h((1-r)/2) - \ln 2] - h((2-r)/4)$ .

In addition, the QSL time in Eq. (27) related to the quantum Jensen-Shannon distance becomes

$$\begin{aligned} \frac{\tau_{JS}^{\text{QSL}}}{\tau} &= \frac{2r}{3} \left[ h\left(\frac{1-r}{2}\right) + h\left(\frac{1-r_\tau^D}{2}\right) - 2h\left(\frac{1-r_\tau^D}{2}\right) \right] \\ &\times \left\{ (2 + \ln 2)(r - r_\tau^D) - (1 - r_\tau^D) \ln[(1 - r_\tau^D)/4] \right. \\ &\left. - (2 - r - r_\tau^D) \ln(2 - r - r_\tau^D) + 3(1 - r) \ln(1 - r) \right\}^{-1}. \end{aligned} \quad (37)$$

From Eq. (37), we find that the ratio  $\tau_{JS}^{\text{QSL}}/\tau$  is independent of the angular coordinates  $\theta$  and  $\phi$  of the Bloch sphere. We find the ratio  $\tau_{JS}^{\text{QSL}}/\tau \rightarrow 0$  for  $\Gamma\tau \rightarrow 0$ , while for  $\Gamma\tau \gg 1$  we have that the QSL time approaches a time-independent quantity that exclusively depends on the mixedness parameter  $r \in [0, 1)$ . It turns out that  $\tau_{JS}^{\text{QSL}}/\tau \rightarrow 0$  for  $r \rightarrow 0$ , regardless  $\Gamma\tau \geq 0$ .

In Fig. 2, we plot the speed limits  $\tau_{J,J_S}^{\text{QSL}}$  [see Figs. 2(a) and 2(c)] and the normalized relative errors  $\tilde{\delta}_{J,J_S}(\tau)$  [see Figs. 2(b) and 2(d)], as a function of the mixedness parameter  $r$  and the dimensionless parameter  $\Gamma\tau$ , for initial single-qubit states evolving under the depolarizing channel. Figures 2(a) and 2(c) show that, respectively,  $\tau_J^{\text{QSL}}$  [see Eq. (35)] and  $\tau_{JS}^{\text{QSL}}$  [see Eq. (37)] exhibit similar qualitative behavior, thus being monotonic functions of the parameters  $r$  and  $\Gamma\tau$ . In both cases, for a fixed value  $r \in [0, 1)$  ( $\Gamma\tau \geq 0$ ), the QSL time  $\tau_{J,J_S}^{\text{QSL}}$  increases monotonically as a function of  $\Gamma\tau \geq 0$  ( $0 \leq r < 1$ ). In particular, for  $0 \leq r \lesssim 0.2$ , one finds that  $\tau_{J,J_S}^{\text{QSL}}$  approaches

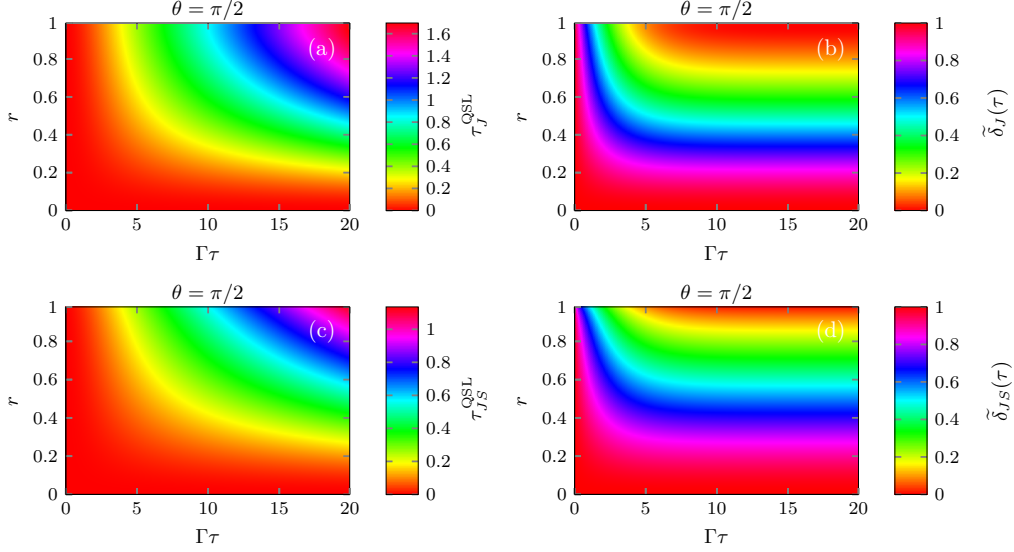


FIG. 3. (Color online) Density plot of the entropic QSLs  $\tau_{J,S}^{\text{QSL}}$  [see Eqs. (26) and (27), respectively], and the normalized relative errors  $\tilde{\delta}_{J,S}(\tau)$  [see Eq. (33)], as a function of the dimensionless parameters  $\Gamma\tau$  and  $r \in [0, 1)$ , for initial single-qubit states subject to the phase damping quantum channel [see Sec. VB 2]. Here, we set  $\theta = \pi/2$ , for all  $\phi \in [0, 2\pi)$ .

small values for the overall dynamics. This means that the closer the initial state is to the center of the Bloch sphere, the faster the system evolves towards to the maximally mixed state.

Figures 2(b) and 2(d) show that  $\tilde{\delta}_{J,S}(\tau)$  presents similar qualitative behavior for both QJPD and QJSD measures. We note that, for a fixed value  $\Gamma\tau \geq 0$ , then  $\tilde{\delta}_{J,S}(\tau)$  monotonically decreases as a function of  $r$ . In particular, for  $0.9 \lesssim r < 1$  and  $\Gamma\tau \gtrsim 3$ , one finds that the normalized relative errors approaches small values  $\tilde{\delta}_{J,S}(\tau) \approx 0$ . This suggests that the closer the initial state is to a pure state, that is, the further it is from the fixed point of the nonunitary dynamics, the tighter the bounds will be. Otherwise, the bounds are looser for initial states close to the maximally mixed state, regardless of  $\Gamma\tau \geq 0$ . We note that, for a given fixed value  $0 \leq r < 1$ , each relative error approaches a certain value that remains constant at later times of the dynamics.

## 2. Phase damping channel

The phase damping channel is described by the Kraus operators  $K_0 = |0\rangle\langle 0| + \sqrt{1-\lambda_t}|1\rangle\langle 1|$ , and  $K_1 = \sqrt{\lambda_t}|1\rangle\langle 1|$ , where  $\{|0\rangle, |1\rangle\}$  is the computational basis states, with  $\lambda_t = 1 - e^{-\Gamma t}$ , and  $\Gamma$  is the decoherence rate [35]. This is also a unital quantum channel, which in turn describes the loss of coherence of open quantum systems without energy dissipation. In this case, the energy spectrum of the system remains unchanged, while its eigenstates accumulate a relative phase that is destroyed during the nonunitary evolution.

The evolved state of the two-level system is given

by  $\rho_t^{PD} = \sum_{j=0}^1 K_j \rho_0 K_j^\dagger = (1/2) (\mathbb{I} + \vec{r}_t^{PD} \cdot \vec{\sigma})$ , with  $\vec{r}_t^{PD} = \eta_t^{PD} \vec{r}$ , where  $\eta_t^{PD} = \text{diag}(\sqrt{1-\lambda_t}, \sqrt{1-\lambda_t}, 1)$  is a real-valued, diagonal matrix. For  $\Gamma t \gg 1$ , one obtains the asymptotic vector  $\vec{r}_\infty^{PD} \approx (0, 0, r \cos \theta)$  related to the stationary state  $\rho_\infty^{PD} \approx (1/2)((1+r \cos \theta)|0\rangle\langle 0| + (1-r \cos \theta)|1\rangle\langle 1|)$ . The latter is an incoherent state with respect to the computational basis  $\{|0\rangle, |1\rangle\}$ , i.e., the complete set of eigenvectors of the observable  $\sigma_z$ . The instantaneous state exhibits the eigenvalues  $\kappa_{\max/\min}(\rho_t^{PD}) = (1 \pm r_t^{PD})/2$ , with

$$r_t^{PD} = r \sqrt{1 - \lambda_t \sin^2 \theta}. \quad (38)$$

In turn, for the convex combination  $\varpi_t^{PD} = (1/2)(\rho_0 + \rho_t^{PD})$ , we find the time-dependent eigenvalues  $\kappa_{\max/\min}(\varpi_t^{PD}) = (1/2)(1 \pm \nu_t^{PD})$ , with

$$\nu_t^{PD} = r \sqrt{1 - \frac{1}{4} \left( \lambda_t + 2 \left( 1 - \sqrt{1 - \lambda_t} \right) \right) \sin^2 \theta}. \quad (39)$$

In this setting, we find the analytical expression for the quantum Jeffreys pseudo-distance given as follows

$$D_J(\rho_0, \rho_\tau^{PD}) = \frac{\sin \theta}{2} \sqrt{r \left( 1 - \sqrt{1 - \lambda_\tau} \right)} \left[ \ln \left( \frac{1+r}{1-r} \right) - \frac{r}{r_\tau^{PD}} \sqrt{1 - \lambda_\tau} \ln \left( \frac{1+r_\tau^{PD}}{1-r_\tau^{PD}} \right) \right]^{1/2}. \quad (40)$$

Equation (40) shows that the quantum Jeffreys pseudo-distance does not depend on the initial azimuth angle  $\phi$ . We note that QJPD vanishes for incoherent probe states with  $\theta = 0$  that belong to the  $z$ -axis of the Bloch sphere. On the one hand, for

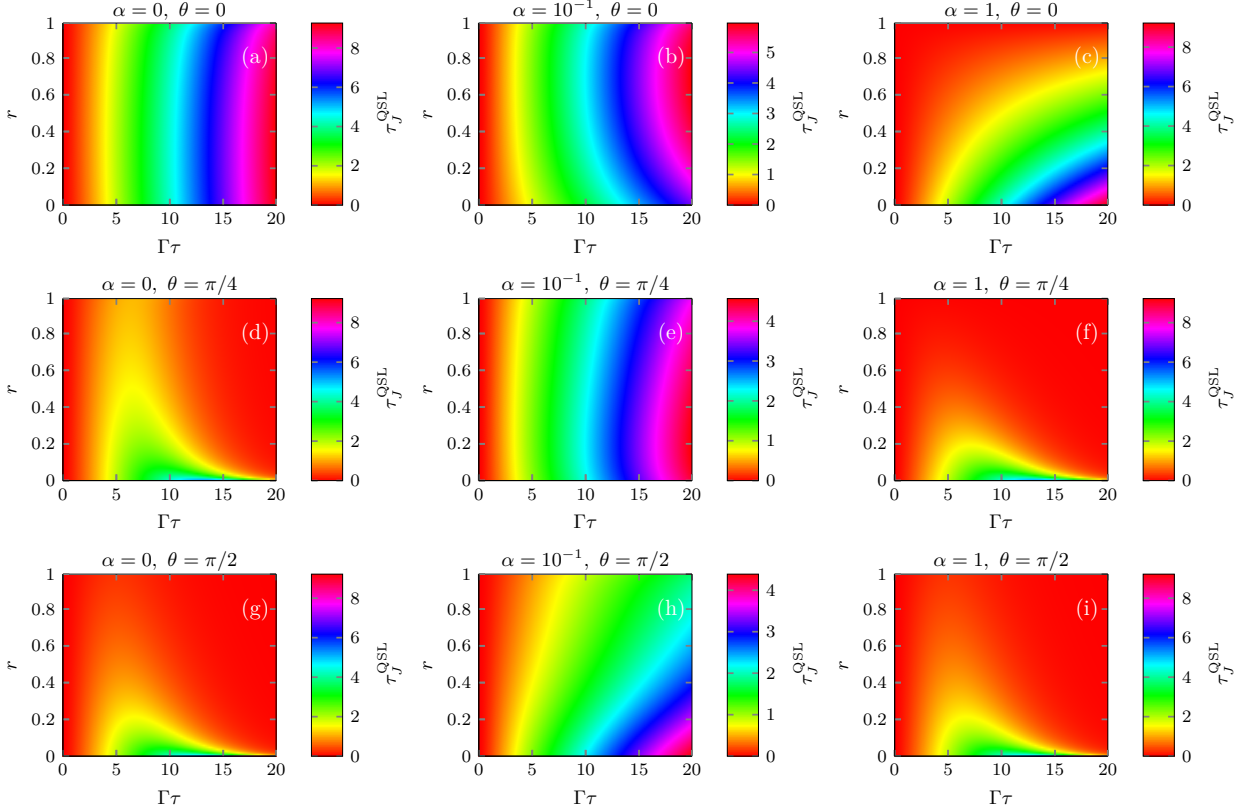


FIG. 4. (Color online) Density plot of the entropic QSL  $\tau_J^{\text{QSL}}$  [see Eq. (26)], as a function of the dimensionless parameters  $\Gamma\tau$  and  $r \in [0, 1]$ , for initial single-qubit states subject to the generalized amplitude damping channel [see Sec. VB 3]. Here, we set  $\alpha = \{0, 0.1, 1\}$  and  $\theta = \{0, \pi/4, \pi/2\}$ , for all  $\phi \in [0, 2\pi]$ .

$\Gamma\tau \ll 1$ , we find that QJPD becomes  $D_{JS}^2(\rho_0, \rho_\tau^{PD}) \approx (r/32)(\Gamma\tau)^2 \sin^2(2\theta) \{ (1/2) \ln[(1+r)/(1-r)] + r \tan^2\theta / (1-r^2) \}$ , which in turn scales quadratically with the dimensionless parameter  $\Gamma\tau$ . On the other hand, for  $\Gamma\tau \gg 1$ , QJPD approaches the asymptotic value  $D_{JS}^2(\rho_0, \rho_\tau^{PD}) \approx (r/4) \sin^2\theta \ln[(1+r)/(1-r)]$ , which is time-independent.

In turn, one finds that the quantum Jensen-Shannon distance is given by

$$D_{JS}(\rho_0, \rho_\tau^{PD}) = \frac{1}{\sqrt{2}} \sqrt{h\left(\frac{1-r_\tau^{PD}}{2}\right) + h\left(\frac{1-r}{2}\right) - 2h\left(\frac{1-\nu_\tau^{PD}}{2}\right)}. \quad (41)$$

On the one hand, for  $\Gamma\tau \ll 1$ , one verifies that  $D_{JS}^2(\rho_0, \rho_\tau^{PD}) \approx (r/128)(\Gamma\tau)^2 \sin^2(2\theta) \{ (1/2) \ln[(1+r)/(1-r)] + r \tan^2\theta / (1-r^2) \}$ , i.e., the squared QJSD increases quadratically with the dimensionless parameter  $\Gamma\tau$ . On the other hand, for  $\Gamma\tau \gg 1$ , QJSD approaches the time-independent value  $D_{JS}^2(\rho_0, \rho_\tau^{PD}) \approx (1/2)[h((1-r \cos\theta)/2) + h((1-r)/2) - 2h((2-r\sqrt{4-3\sin^2\theta})/4)]$ .

The entropic QSL times  $\tau_{J,JS}^{\text{QSL}}$  related to QJPD and QJSD are evaluated through Eqs. (26) and (27), respectively. The expressions are too long to be reported here.

We note that the cost functions  $f_{J,JS}(\rho_0, \rho_t^{PD})$  are given by Eqs. (8) and (9), respectively. In Table I, we show useful information-theoretic parameters needed to compute  $\tau_{J,JS}^{\text{QSL}}$  for initial single-qubit states evolving under the phase damping quantum channel. Overall, one arrives at trivial bounds  $\tau_{J,JS}^{\text{QSL}} \approx 0$  for initial states belonging to the  $z$  axis of the Bloch sphere, since they are invariant under the quantum operation.

In Fig. 3, we show the density plots of the entropic QSL time  $\tau_{J,JS}^{\text{QSL}}$  [see Figs. 3(a) and 3(c)], and the normalized relative error  $\tilde{\delta}_{J,JS}(\tau)$  [see Figs. 3(b) and 3(d)], as a function of the dimensionless parameters  $\Gamma\tau$  and  $r$ , for single-qubit states evolving under the phase damping channel. Here we set initial states with  $\theta = \pi/2$  lying in the equatorial plane of the Bloch sphere. Figures 3(a) and 3(c) show that  $\tau_J^{\text{QSL}}$  and  $\tau_{JS}^{\text{QSL}}$  exhibit the same qualitative behavior, monotonically increasing as a function of  $\Gamma\tau$  and  $r$ . It is worth noting that  $\tau_{J,JS}^{\text{QSL}}$  approaches small values at earlier times of the dynamics ( $0 \leq \Gamma\tau \lesssim 2$ ), regardless of the purity of the initial state. In addition, for all  $\Gamma\tau \geq 0$ , the less pure the probe state, the smaller the entropic speed limit time.

In Figs. 3(b) and 3(d), we plot the normalized relative errors  $\tilde{\delta}_{J,JS}(\tau)$  as a function of the dimensionless para-

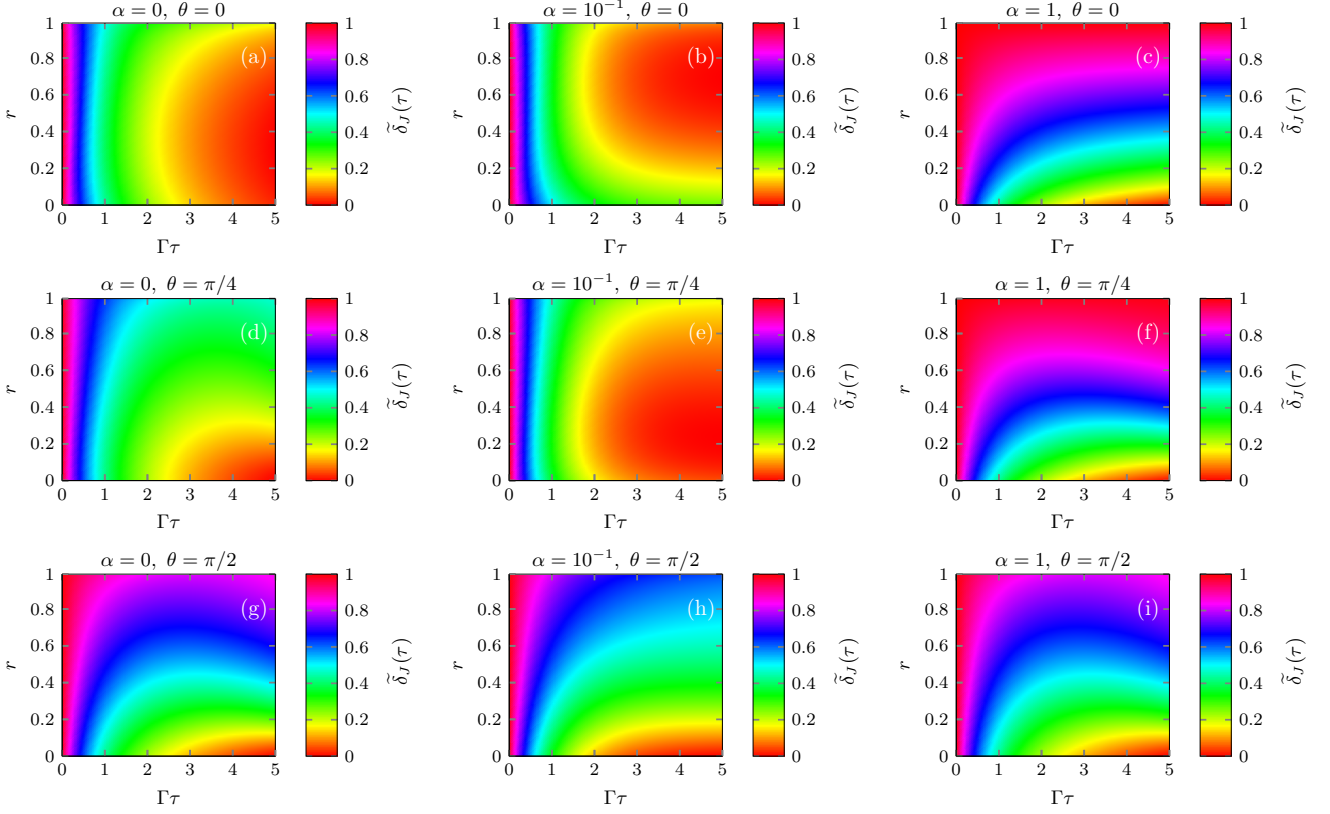


FIG. 5. (Color online) Density plot of the normalized relative error  $\tilde{\delta}_J(\tau)$  [see Eq. (33)], as a function of the dimensionless parameters  $\Gamma\tau$  and  $r \in [0, 1]$ , for initial single-qubit states subject to the generalized amplitude damping channel [see Sec. VB 3]. Here, we set  $\alpha = \{0, 0.1, 1\}$  and  $\theta = \{0, \pi/4, \pi/2\}$ , for all  $\phi \in [0, 2\pi)$ .

parameters  $\Gamma\tau$  and  $r$ . On the one hand, for fixed  $\Gamma\tau \geq 0$ , one finds that  $\tilde{\delta}_{J,JS}(\tau)$  decreases as a function of the mixedness parameter  $r \in [0, 1]$ . On the other hand, for fixed  $r \gtrsim 0.2$ , we have that  $\tilde{\delta}_{J,JS}(\tau)$  monotonically decreases as a function of  $\Gamma\tau$ , and approaches a constant value at later times of the dynamics. The closer the probe state is to the maximally mixed state, the looser the bounds will be, for all  $\Gamma\tau \geq 0$ . We note that  $\tilde{\delta}_{J,JS}(\tau)$  approaches small values at later times of the dynamics for initial states with purity close to the unity.

### 3. Generalized amplitude damping channel

The generalized amplitude damping channel (GAD) describes the dissipative dynamics of a two-level system in contact with a thermal bath at finite temperature. The GAD channel models the energy loss from the two-level system to the thermal bath, accounting for excitations between ground and excited states at finite temperature [120, 121]. The quantum channel is modeled by the Kraus operators  $K_0 = \sqrt{\alpha}|0\rangle\langle 0| + \sqrt{1-\lambda_t}|1\rangle\langle 1|$ ,  $K_1 = \sqrt{\alpha\lambda_t}|0\rangle\langle 1|$ ,  $K_2 = \sqrt{1-\alpha}(\sqrt{1-\lambda_t}|0\rangle\langle 0| + |1\rangle\langle 1|)$ , and  $K_3 = \sqrt{(1-\alpha)\lambda_t}|1\rangle\langle 0|$ , with  $\lambda_t = 1 - e^{-\Gamma t}$ , where

$1/\Gamma$  is the characteristic time of the dissipative process [35]. The parameter  $\alpha \in [0, 1]$  encodes the temperature effects of the noisy dynamics, with  $\alpha = 0$  ( $\alpha = 1$ ) respective to the case of infinite (zero) temperature. In particular, for  $\alpha = 1$ , GAD channel reduces to the standard amplitude damping channel [120].

In this setting, the evolved state becomes  $\rho_t^{GAD} = \sum_{j=0}^3 K_j \rho_0 K_j^\dagger = (1/2)(\mathbb{I} + \vec{r}_t^{GAD} \cdot \vec{\sigma})$ , with  $\vec{r}_t^{GAD} = \eta_t^{GAD} \vec{r} + \vec{\kappa}_t^{GAD}$ , where  $\eta_t^{GAD} = \text{diag}(\sqrt{1-\lambda_t}, \sqrt{1-\lambda_t}, 1-\lambda_t)$  is a diagonal matrix, while  $\vec{\kappa}_t^{GAD} = (0, 0, (2\alpha-1)\lambda_t)$  is a real-valued tridimensional vector. In particular, for  $\Gamma t \gg 1$ , one finds the asymptotic vector  $\vec{r}_\infty^{GAD} \approx (0, 0, 2\alpha-1)$ , which in turn describes the stationary, mixed, single-qubit state  $\rho_\infty^{GAD} \approx \alpha|0\rangle\langle 0| + (1-\alpha)|1\rangle\langle 1|$ . This means that the GAD channel shrinks the Bloch sphere along the  $z$ -axis towards to a fixed point located at  $z = 2\alpha - 1$  [35].

The instantaneous state exhibits the eigenvalues  $\kappa_{\max/\min}(\rho_t^{GAD}) = (1/2)(1 \pm r_t^{GAD})$ , with

$$r_t^{GAD} = \sqrt{[(2\alpha-1)\lambda_t + (1-\lambda_t)r \cos \theta]^2 + (1-\lambda_t)r^2 \sin^2 \theta}. \quad (42)$$

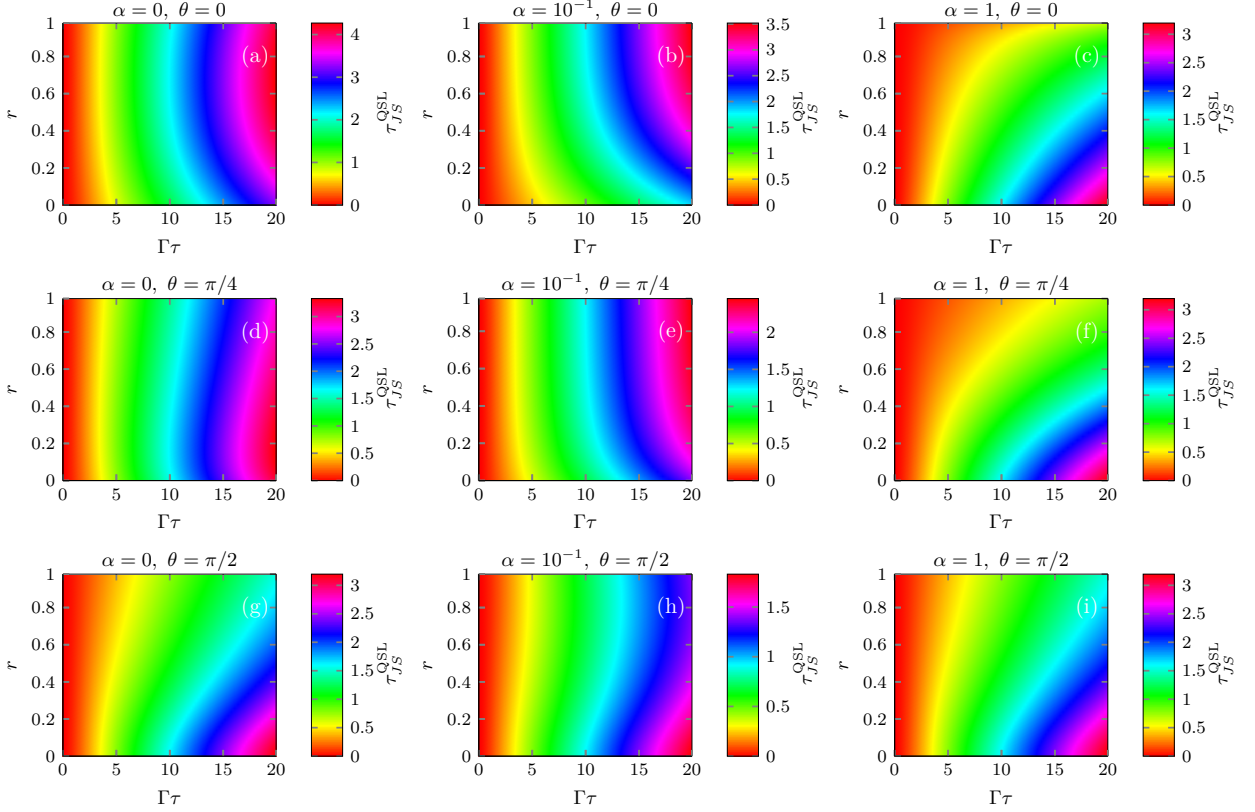


FIG. 6. (Color online) Density plot of the entropic QSL  $\tau_{JS}^{\text{QSL}}$  [see Eq. (27)], as a function of the dimensionless parameters  $\Gamma\tau$  and  $r \in [0, 1]$ , for initial single-qubit states subject to the generalized amplitude damping channel [see Sec. VB 3]. Here, we set  $\alpha = \{0, 0.1, 1\}$  and  $\theta = \{0, \pi/4, \pi/2\}$ , for all  $\phi \in [0, 2\pi)$ .

In particular, for  $\Gamma t \gg 1$  (or  $t \rightarrow \infty$ ), Eq. (42) approaches the value  $r_\infty^{\text{GAD}} \approx |2\alpha - 1|$ , which in turn depicts the asymptotic state of the Markovian dynamics, while for  $t = 0$  one finds that  $r_0^{\text{GAD}} = r$ , thus recovering the initial state of the system, as expected. For the convex combination  $\varpi_t^{\text{GAD}} = (1/2)(\rho_0 + \rho_t^{\text{GAD}})$ , we find the set of eigenvalues  $\kappa_{\text{max/min}}(\varpi_t^{\text{GAD}}) = (1/2)(1 \pm \nu_t^{\text{GAD}})$ , with

$$\begin{aligned} \nu_t^{\text{GAD}} = & \frac{1}{2} \{ \lambda_t(2\alpha - 1) (2(2 - \lambda_t)r \cos \theta + \lambda_t(2\alpha - 1)) \\ & + r^2 [(2 - (2 - \lambda_t)\sqrt{1 - \lambda_t})\sqrt{1 - \lambda_t} \sin^2 \theta \\ & + (2 - \lambda_t)^2] \}^{1/2}. \end{aligned} \quad (43)$$

In particular, for  $t = 0$ , Eq. (43) reduces to  $\nu_0^{\text{GAD}} = r$ , which agrees with the fact that  $\varpi_0^{\text{GAD}} = \rho_0$  recovers the initial state. Furthermore, for  $\Gamma t \gg 1$ , we have that  $\nu_\infty^{\text{GAD}} \approx (1/2)\sqrt{(r \cos \theta + 2\alpha - 1)^2 + r^2 \sin^2 \theta}$ . This indicates that the states  $\rho_0$  and  $\rho_\infty$  do not commute with each other, and the asymptotic eigenvalues  $\kappa_{\text{max/min}}(\varpi_\infty^{\text{GAD}})$  still depend on the parameters  $(r, \theta, \alpha)$ .

Based on these results, it follows that the quantum Jeffreys pseudo-distance for the single-qubit states  $\rho_0$  and

$\rho_\tau^{\text{GAD}}$  can be analytically evaluated as follows

$$\begin{aligned} D_J(\rho_0, \rho_\tau^{\text{GAD}}) = & \frac{1}{2} \left\{ \xi_\tau \ln \left( \frac{1+r}{1-r} \right) \right. \\ & \left. + \left( r_\tau^{\text{GAD}} + \frac{r(\xi_\tau - r)}{r_\tau^{\text{GAD}}} \right) \ln \left( \frac{1+r_\tau^{\text{GAD}}}{1-r_\tau^{\text{GAD}}} \right) \right\}^{1/2}, \end{aligned} \quad (44)$$

where we introduce the auxiliary parameter  $\xi_\tau := r(1 - \sqrt{1 - \lambda_\tau})(1 + \sqrt{1 - \lambda_\tau} \cos^2 \theta) - (2\alpha - 1)\lambda_\tau \cos \theta$ . In turn, the quantum Jensen-Shannon distance for  $\rho_0$  and  $\rho_\tau^{\text{GAD}}$  is given by

$$\begin{aligned} D_{JS}(\rho_0, \rho_\tau^{\text{GAD}}) = & \frac{1}{\sqrt{2}} \sqrt{h \left( \frac{1 - r_\tau^{\text{GAD}}}{2} \right) + h \left( \frac{1 - r}{2} \right) - 2h \left( \frac{1 - \nu_\tau^{\text{GAD}}}{2} \right)}. \end{aligned} \quad (45)$$

It is noteworthy that, for all  $0 \leq r < 1$  and  $\Gamma\tau > 0$ , we have that  $D_{J,JS}(\rho_0, \rho_\tau^{\text{GAD}})$  remains invariant under the mapping  $(\theta, \alpha) \rightarrow (\theta \pm \pi, 1 - \alpha)$ , with  $\theta \in [0, \pi]$  and  $0 \leq \alpha \leq 1$ . This property is inherited from Eqs. (42) and (43), which means that the eigenvalues  $\kappa_{\text{max/min}}(\rho_t^{\text{GAD}})$  and  $\kappa_{\text{max/min}}(\varpi_t^{\text{GAD}})$  exhibit such a symmetry.

The entropic QSL times  $\tau_{J,JS}^{\text{QSL}}$  related to the QJPD and QJSD are evaluated through Eqs. (26) and (27),

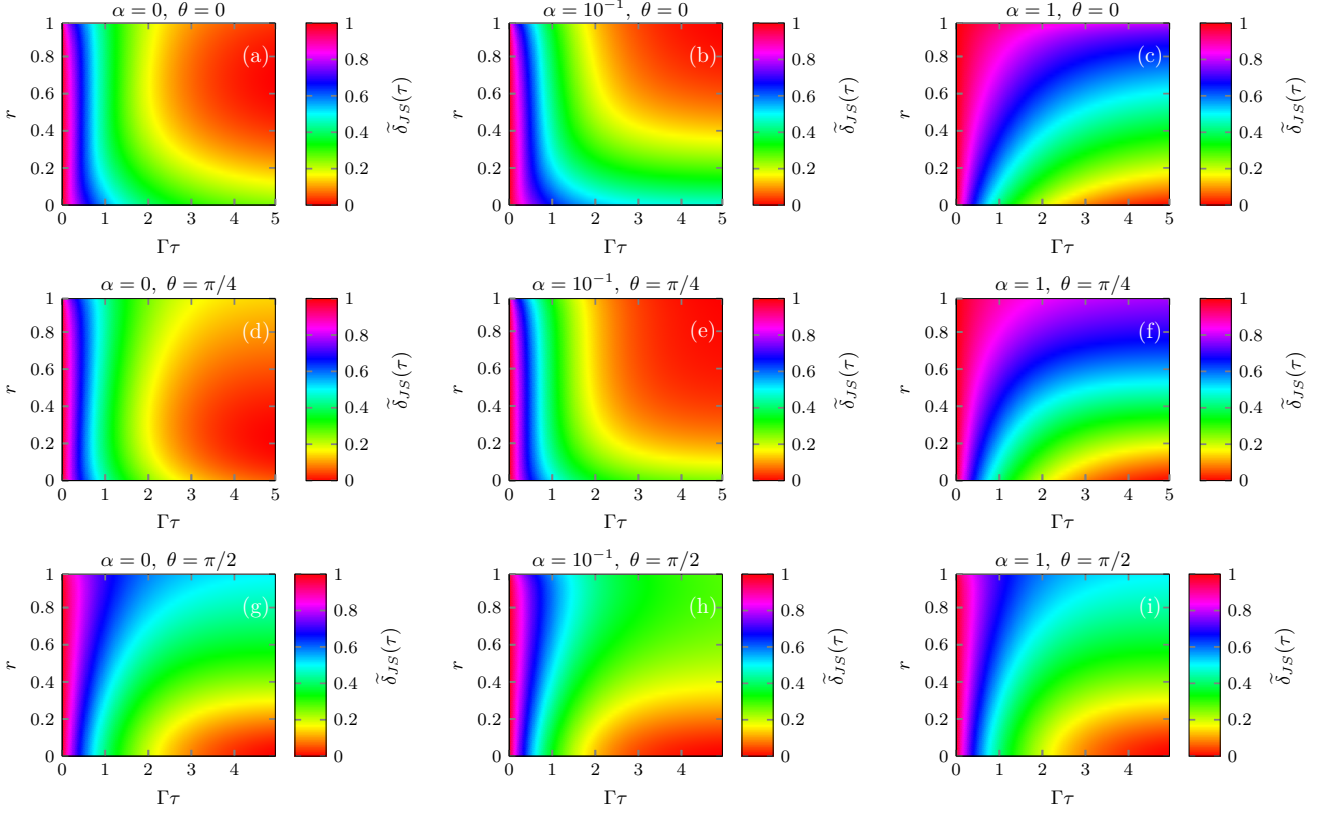


FIG. 7. (Color online) Density plot of the normalized relative error  $\tilde{\delta}_{J,S}(\tau)$  [see Eq. (33)], as a function of the dimensionless parameters  $\Gamma\tau$  and  $r \in [0, 1]$ , for initial single-qubit states subject to the generalized amplitude damping channel [see Sec. VB 3]. Here, we set  $\alpha = \{0, 0.1, 1\}$  and  $\theta = \{0, \pi/4, \pi/2\}$ , for all  $\phi \in [0, 2\pi)$ .

respectively. The expressions are too long to be reported here. In Table I, we show some useful quantities needed to compute  $\tau_{J,J_S}^{\text{QSL}}$  for initial single-qubit states evolving under the generalized amplitude damping channel. We remind that the cost functions  $f_{J,J_S}(\rho_0, \rho_t^{\text{GAD}})$  are given in Eqs. (8) and (9), respectively. It turns out that  $\tau_{J,J_S}^{\text{QSL}}$  and  $\tilde{\delta}_{J,J_S}(\tau)$  are symmetric under the mapping  $(\theta, \alpha) \rightarrow (\theta \pm \pi, 1 - \alpha)$ , this being an inherited property from QJPD and QJSD. In other words, given two probe states with  $(r, \theta_1, \phi, \alpha_1)$  and  $(r, \theta_2, \phi, \alpha_2)$ , one expects to obtain the same QSL time whenever we have  $|\theta_{1(2)} - \theta_{2(1)}| = \pi$  and  $\alpha_1 + \alpha_2 = 1$ , for all  $\Gamma\tau > 0$ .

Hereafter, we analyze numerical simulations of the entropic QSL times  $\tau_{J,J_S}^{\text{QSL}}$  and the normalized relative errors  $\tilde{\delta}_{J,J_S}(\tau)$  for single-qubit states evolving under the GAD channel. We set probe states with  $\theta = \{0, \pi/4, \pi/2\}$ , regardless of the azimuth angle  $\phi \in [0, 2\pi)$ , and also consider the parameters  $\alpha = \{0, 0.1, 1\}$ .

In Fig. 4, we show the density plots of the entropic QSL time  $\tau_J^{\text{QSL}}$ , as a function of the dimensionless parameters  $\Gamma\tau$  and  $r$ . We note that, for a fixed value  $r \in [0, 1)$  of the mixedness parameter, with  $\alpha = 0.1$  and  $\theta = \{0, \pi/4, \pi/2\}$ , then  $\tau_J^{\text{QSL}}$  monotonically increases as a function of the dimensionless parameter  $\Gamma\tau \geq 0$  [see

Figs. 4(b), 4(e), and 4(h)]. In particular, for  $\alpha = 0$  and  $\alpha = 1$ , with  $\theta = \{\pi/4, \pi/2\}$ , we have that the entropic QSL approaches small values at earlier ( $\Gamma\tau \ll 1$ ) and later ( $\Gamma\tau \gg 1$ ) times of the dynamics for initial mixed states, regardless  $0 < r < 1$  [see Figs. 4(d), 4(f), 4(g), and 4(i)]. In this setting, one finds that  $\tau_J^{\text{QSL}}$  exhibits a non-monotonic behavior as a function of  $\Gamma\tau$  along the nonunitary evolution of the two-level system. Indeed, Figs. 4(d), 4(f), 4(g), and 4(i) show that, for fixed value  $r \in [0, 1)$ , the QSL time starts growing but smoothly approaches small values as a function of  $\Gamma\tau \geq 0$ . It is noteworthy that, for  $\alpha = \{0, 1\}$  and  $\theta = \pi/2$ ,  $\tau_J^{\text{QSL}}$  [see Eq. (26)] exhibits the same quantitative behavior, which can be numerically verified in Figs. 4(g) and 4(i).

In Fig. 5, we show the density plots of the normalized relative error  $\tilde{\delta}_J(\tau)$ , as a function of the dimensionless parameters  $\Gamma\tau$  and  $r$ . The entropic QSL bound is loose at earlier times of the dynamics, regardless of the initial state and the value of the parameter  $\alpha \in [0, 1]$ . In addition, Figs. 5(c) and 5(f) show that the bound is also loose for probe states close to the incoherent state  $|0\rangle\langle 1|$ , for all  $\Gamma\tau \geq 0$ . Overall, for  $\alpha \ll 1$  and  $\theta = \{0, \pi/4, \pi/2\}$ , one finds that  $\tilde{\delta}_J(\tau)$  approaches small values for all  $\Gamma\tau \gg 1$  [see Figs. 5(a), 5(b), 5(d), 5(e), 5(g), and 5(h)]. In par-

ticular, for  $\theta = \pi/2$ , tighter entropic QSLs are found at later times of the dynamics whenever the initial state is close to the maximally mixed state, regardless the value of  $\alpha = \{0, 0.1, 1\}$  [see Figs. 5(g), 5(h), and 5(i)].

In Fig. 6, we show the density plots of the entropic QSL time  $\tau_{JS}^{\text{QSL}}$ , as a function of the dimensionless parameters  $\Gamma\tau$  and  $r$ . We note that, for a fixed value  $r \in [0, 1)$  of the mixedness parameter,  $\tau_{JS}^{\text{QSL}}$  varies monotonically as a function of the dimensionless parameter  $\Gamma\tau \geq 0$ . Overall, the entropic QSL approaches small values at earlier times of the dynamics, exhibiting similar qualitative behavior regardless the initial state and temperature of the thermal bath that we consider here. In particular, for  $\alpha = \{0, 1\}$  and  $\theta = \pi/2$ , Figs. 6(g) and 6(i) show that the QSL time exhibits the same quantitative behavior. This comes from the fact that  $\tau_{JS}^{\text{QSL}}$  reduces to the same result under this choice of parameters, regardless of  $r \in [0, 1)$  and  $\Gamma\tau \geq 0$  [see Eq. (27)]. This means that, for a given probe mixed state lying in the equatorial plane of the Bloch sphere, with  $0 < r < 1$  and  $\theta = \pi/2$ , the QSL time at which the system reaches the stationary states  $|1\rangle\langle 1|$  ( $\alpha = 0$ ) or  $|0\rangle\langle 0|$  ( $\alpha = 1$ ) will be the same.

In Fig. 7, we show the density plots of the normalized relative error  $\tilde{\delta}_{JS}(\tau)$ , as a function of the dimensionless parameters  $\Gamma\tau$  and  $r$ . We note that, for a fixed value  $r \in [0, 1)$  of the mixedness parameter,  $\tilde{\delta}_{JS}(\tau)$  monotonically decreases as a function of the dimensionless parameter  $\Gamma\tau \geq 0$ . In particular, for  $\Gamma\tau \lesssim 0.25$ , one finds that  $0.8 \lesssim \tilde{\delta}_{JS}(\tau) \lesssim 1$ , with  $r \in [0, 1)$ . This means that the entropic QSL bound is looser at earlier times of the dynamics, regardless of the purity of the initial single-qubit state. Furthermore, we have that  $\tilde{\delta}_{JS}(\tau)$  approaches small values at later times of the dynamics. For example, Figs. 7(c), 7(f), 7(g), 7(h), and 7(i) show that  $\tilde{\delta}_{JS}(\tau) \lesssim 0.2$  for  $0 \leq r \lesssim 0.2$  and  $\Gamma\tau \gtrsim 2$ , with  $\theta = \{0, \pi/4, \pi/2\}$  and  $\alpha = \{0, 0.1, 1\}$ .

## VI. CONCLUSIONS

In this work, we have addressed quantum speed limits based on quantum versions of the Jeffreys divergence and Jensen-Shannon divergence. These distinguishability measures correspond to symmetrizations of the standard quantum relative entropy, also called Umegaki relative entropy. Both are nonnegative, symmetric with respect to the swap of the two input states, contractive under the action of completely positive and trace-preserving maps, but do not satisfy triangle inequality. So far, the square root of Jensen-Shannon divergence (QJSD) has proven to be a *bona fide* information metric on the convex manifold of quantum states, but there is no clear evidence that square root of the Jeffreys divergence (QJPD) also shares such this property. We study QJPD and QJSD to obtain entropic QSLs that apply to finite-dimensional quantum systems undergoing general physical processes.

We investigate the dynamical behavior of QJPD and QJSD evaluated for states of arbitrary quantum systems, thus proving upper bounds on these quantities [see Eqs. (14) and (19)]. The bounds are evaluated in terms of the Schatten speed of the instantaneous state, as well as cost functions that depend on the smallest and largest eigenvalues of both initial and instantaneous states of the quantum system [see Eqs. (8) and (9)]. These bounds are expected to require low computational efforts, mainly because their evaluation involves few eigenvalues of the probe and evolved states, thus providing useful estimates of QJSD and QJPD for higher-dimensional quantum systems. In particular, using Pinsker's inequality, we present an inequality that establishes lower and upper bounds on QJPD [see Eq. (15)].

We address entropic QSLs based on QJPD [see Eq. (20)] and QJSD [see Eq. (23)], which apply for both closed and open quantum systems. On the one hand, for unitary dynamics, we obtain QSLs from QJPD [see Eq. (24)] and QJSD [see Eq. (25)] that depend on the Schatten 1-norm of the commutator between the probe state and the Hamiltonian that generates the dynamics. This quantity signals the role played by the coherences of the initial state with respect to the fixed eigenbasis of the Hamiltonian. In this setting, one readily verifies that the QSLs are inversely proportional to the variance of the time-independent Hamiltonian, i.e., our results fit into the class of Mandelstam-Tamm speed limits. On the other hand, for nonunitary evolutions described by CPTP maps, we derive entropic QSLs from QJPD [see Eq. (26)] and QJSD [see Eq. (27)] written in terms of the Kraus operators that describes the overall evolution.

To illustrate our findings, we have specialized these results to the case of two-level systems undergoing (i) unitary dynamics [see Sec. VA], and (ii) nonunitary dynamics [see Sec. VB]. On the one hand, for closed quantum systems, we consider the unitary evolution of mixed single-qubit states generated by a time-independent Hamiltonian. We obtain analytical QSLs based on QJPD [see Eq. (30)] and QJSD [see Eq. (31)], also discussing their dynamical properties. On the other hand, for open quantum systems, we set the nonunitary dynamics generated by three quantum operations, namely, depolarizing channel, phase damping channel, and generalized amplitude damping channel. We provide analytical results for QJPD and QJSD in each case, and also present numerical simulations to support our findings about QSLs [see Figs. 2, 3, 4, and 6]. We also address the tightness of these speed limits [see Figs. 2, 3, 5, and 7]. The bounds are looser at earlier times of the dynamics, and they are not tight for the overall evolution.

It is worth mentioning that entropic QSLs based on  $\alpha$ -z-Rényi relative entropies were recently presented in Ref. [34]. Hence, it is natural to ask in what extent such results can or can not overcome the bounds discussed here, particularly since it would be possible to recover Umegaki's relative entropy from  $\alpha$ -z-Rényi relative entropies by choosing  $z = 1$ , and taking the limit

$\alpha \rightarrow 1$ . We point out that the results discussed here are not compatible with those addressed in Ref. [34]. First, the results in Ref. [34] does apply only for  $\alpha \in (0, 1)$  and  $1 \geq z \geq \max\{\alpha, 1 - \alpha\}$ , with  $\alpha \neq 1$ , which rules out any chance of obtaining QSLs based on standard relative entropy from  $\alpha$ - $z$ -Rényi relative entropies. This means that the bounds presented here cannot be recovered from the results in Ref. [34], neither as particular cases nor as straightforward applications. Second, the number of inequalities used can actually lead to different families of bounds, which also undermines the tightness of these quantities. Indeed, tighter bounds on QJPD and QJSD are expected by applying a small number of inequalities, which may imply tighter and attainable speed limits. Leveraging the sensitivity of our QSLs respective to a few eigenvalues of the system overcomes the need to evaluate the full spectrum of effective Liouvillians in open quantum systems, which is the case of Refs. [9, 32, 33] that showed QSLs based on relative entanglement entropies.

We emphasize that our bounds require minimal information about the physical system, e.g., the smallest and largest eigenvalues of the initial and evolved states, and also details about the generator of the dynamics. The entropic QSLs for the nonunitary dynamics of single-qubit states can be experimentally validated using nuclear spins in nuclear magnetic resonance (NMR) setups, following an experimental procedure analogous to that described in Ref. [79]. In turn, for unitary dynamics of two-level systems, the bounds could be analyzed experimentally using moments of energy spectra and quantum state tomography from photonic states in superconducting circuits, according to Refs. [80, 81]. These two proposals deserve further investigation. The results can be useful in the study of entropic uncertainty relations [70, 122], particularly based on Jensen-Shannon and Jeffreys divergences. Our results also may find applications in quantum thermodynamics [123], noisy quantum metrology [124], and also in the study of complexity in quantum many-body quantum dynamics [125].

## ACKNOWLEDGMENTS

This work was supported by the Brazilian ministries MEC and MCTIC, and the Brazilian funding agencies CNPq, and Coordenação de Aperfeiçoamento de Pessoal de Nível Superior–Brasil (CAPES) (Finance Code 001). D. P. P. would like to acknowledge the Fundação de Amparo à Pesquisa e ao Desenvolvimento Científico e Tecnológico do Maranhão (FAPEMA).

## APPENDIX

### A. LOGARITHM OF DENSITY MATRICES

In this Appendix, we address the proof of the integral representation of the logarithm of density matrices as

follows

$$\ln \rho = \int_0^\infty du \left( \frac{1}{1+u} \mathbb{I} - (\rho + u\mathbb{I})^{-1} \right), \quad (\text{A1})$$

where  $\mathbb{I}$  is the identity matrix, and  $\mathcal{S} = \{\rho \in \mathcal{H} \mid \rho^\dagger = \rho, \rho \geq 0, \text{Tr}(\rho) = 1\}$  defines the convex subspace of a  $d$ -dimensional Hilbert space  $\mathcal{H}$ , with  $d = \dim \mathcal{H}$ . To do so, let  $\rho = \sum_j p_j |j\rangle\langle j|$  be a nonsingular, full rank density matrix, where  $\{p_j\}_{j=1,\dots,d}$  and  $\{|j\rangle\}_{j=1,\dots,d}$  define the sets of eigenvalues and eigenstates, respectively. We note that  $0 < p_j < 1$  and  $\sum_j p_j = 1$ ,  $\langle j|\ell\rangle = \delta_{j\ell}$  and  $\sum_j |j\rangle\langle j| = \mathbb{I}$ , where  $\mathbb{I}$  is the identity matrix. Hence, by exploiting the aforementioned spectral decomposition of the density matrix, one gets

$$\ln \rho = \sum_j \ln p_j |j\rangle\langle j|. \quad (\text{A2})$$

We note that the function  $\ln p_j$  exhibits a monotonic behavior as a function of the parameter  $0 < p_j < 1$ , for all  $j = \{1, \dots, d\}$ , and can be written as in terms of the following representation [114, 126]

$$\ln p_j = \int_0^\infty du \left( \frac{1}{1+u} - \frac{1}{p_j+u} \right). \quad (\text{A3})$$

Hence, by combining Eqs. (A2) and (A3), it yields

$$\begin{aligned} \ln \rho &= \int_0^\infty du \left( \frac{1}{1+u} \sum_j |j\rangle\langle j| - \sum_j \frac{1}{p_j+u} |j\rangle\langle j| \right) \\ &= \int_0^\infty du \left( \frac{1}{1+u} \mathbb{I} - \sum_j \frac{1}{p_j+u} |j\rangle\langle j| \right), \end{aligned} \quad (\text{A4})$$

where we have used the completeness relation of the set of eigenstates of the density matrix. It can be also proved that

$$\begin{aligned} (\rho + u\mathbb{I})^{-1} &= \left( \sum_j (p_j + u) |j\rangle\langle j| \right)^{-1} \\ &= \sum_j \frac{1}{p_j + u} |j\rangle\langle j|. \end{aligned} \quad (\text{A5})$$

Finally, combining Eqs. (A4) and (A5), also recognizing the spectral decomposition of the density matrix, we conclude the integral representation of the logarithm of density matrices given in Eq. (A1).

### B. PROOF OF EQ. (11)

In this Appendix, we prove Eq. (11) in the main text, which in turn holds for any time-dependent, nonsingular, full-rank density matrix  $\rho_t \in \mathcal{S}$ . In this setting, the time derivative of the von Neumann entropy

$S(\rho_t) = -\text{Tr}(\rho_t \ln \rho_t)$  is given by

$$\frac{d}{dt} S(\rho_t) = -\text{Tr} \left( \ln \rho_t \frac{d\rho_t}{dt} \right) - \text{Tr} \left( \rho_t \frac{d}{dt} \ln \rho_t \right). \quad (\text{B1})$$

Next, we consider the integral representation of the logarithm of the density matrix  $\rho_t$  as follows [see Eq. (A1)]

$$\ln \rho_t = \int_0^\infty du \left( \frac{1}{1+u} \mathbb{I} - (\rho_t + u\mathbb{I})^{-1} \right). \quad (\text{B2})$$

By taking the time derivative of the previous equation, one gets

$$\frac{d}{dt} \ln \rho_t = \int_0^\infty du (\rho_t + u\mathbb{I})^{-1} \frac{d\rho_t}{dt} (\rho_t + u\mathbb{I})^{-1}, \quad (\text{B3})$$

where we have used that  $d\rho_t^{-1}/dt = -\rho_t^{-1}(d\rho_t/dt)\rho_t^{-1}$ , with  $\rho_t = \rho_t + u\mathbb{I}$  being a nonsingular matrix, i.e.,  $\rho_t^{-1}\rho_t = \rho_t\rho_t^{-1} = \mathbb{I}$ . Hence, by combining Eqs. (B2) and (B3), one gets

$$\begin{aligned} \text{Tr} \left( \rho_t \frac{d}{dt} \ln \rho_t \right) &= \\ &= \int_0^\infty du \text{Tr} \left( \rho_t (\rho_t + u\mathbb{I})^{-1} \frac{d\rho_t}{dt} (\rho_t + u\mathbb{I})^{-1} \right) \\ &= \text{Tr} \left( \rho_t \frac{d\rho_t}{dt} \int_0^\infty du (\rho_t + u\mathbb{I})^{-2} \right), \end{aligned} \quad (\text{B4})$$

where we have applied the identity  $\rho_t(\rho_t + u\mathbb{I})^{-1} = (\rho_t + u\mathbb{I})^{-1}\rho_t$ , and also used the cyclic property of the trace. We consider the spectral decomposition  $\rho_t = \sum_l p_l |l\rangle\langle l|$ , with  $\langle j|l\rangle = \delta_{j,l}$ , while  $0 \leq p_l \leq 1$  and  $\sum_l p_l = 1$ . In this case, one gets

$$\begin{aligned} \int_0^\infty du (\rho_t + u\mathbb{I})^{-2} &= \sum_l \int_0^\infty \frac{du}{(p_l + u)^2} |l\rangle\langle l| \\ &= \sum_l p_l^{-1} |l\rangle\langle l| \\ &= \rho_t^{-1}. \end{aligned} \quad (\text{B5})$$

By substituting Eq. (B5) into Eq. (B4), one gets

$$\begin{aligned} \text{Tr} \left( \rho_t \frac{d}{dt} \ln \rho_t \right) &= \text{Tr} \left( \rho_t \frac{d\rho_t}{dt} \rho_t^{-1} \right) \\ &= \text{Tr} \left( \frac{d\rho_t}{dt} \right) \\ &= 0, \end{aligned} \quad (\text{B6})$$

which follows from the fact that  $\text{Tr}(\rho_t) = 1$ , where we have also used the cyclic property of the trace. Therefore, Eq. (B6) implies that the time derivative of the von Neumann entropy yields

$$\frac{d}{dt} S(\rho_t) = -\text{Tr} \left( \ln \rho_t \frac{d\rho_t}{dt} \right), \quad (\text{B7})$$

and we conclude the proof accordingly.

### C. PROOF OF EQ. (12)

In this Appendix, we prove Eq. (12) in the main text, thus applying for any time-dependent, nonsingular, full-rank density matrix  $\rho_t \in \mathcal{S}$ . We consider the integral representation in Eq. (B3) of the logarithm of the density matrix. Next, we evaluate the following

$$\left| \frac{d}{dt} \text{Tr}(\rho_0 \ln \rho_t) \right| \leq \int_0^\infty du \left| \text{Tr} \left[ (\rho_t + u\mathbb{I})^{-1} \rho_0 (\rho_t + u\mathbb{I})^{-1} \frac{d\rho_t}{dt} \right] \right|, \quad (\text{C1})$$

where we have used that  $|\int du f(u)| \leq \int du |f(u)|$ , and also applied the cyclic property of the trace. By using the matrix norm inequalities  $|\text{Tr}(A_1 A_2 A_3 A_4)| \leq \|A_1 A_2 A_3\|_\infty \|A_4\|_1 \leq \|A_1\|_\infty \|A_2\|_\infty \|A_3\|_\infty \|A_4\|_1$ , one gets the result

$$\begin{aligned} \left| \frac{d}{dt} \text{Tr}(\rho_0 \ln \rho_t) \right| &\leq \\ &\|\rho_0\|_\infty \left\| \frac{d\rho_t}{dt} \right\|_1 \int_0^\infty du \|(\rho_t + u\mathbb{I})^{-1}\|_\infty^2. \end{aligned} \quad (\text{C2})$$

Next, by using that  $\|\rho_0\|_\infty = \kappa_{\max}(\rho_0)$ , and also  $\|(\rho_t + u\mathbb{I})^{-1}\|_\infty = (\kappa_{\min}(\rho_t) + u)^{-1}$ , where  $\kappa_{\min/\max}(\bullet)$  sets the smallest/largest eigenvalue of the referred density matrix, respectively, we obtain the result

$$\begin{aligned} \left| \frac{d}{dt} \text{Tr}(\rho_0 \ln \rho_t) \right| &\leq \\ &\kappa_{\max}(\rho_0) \left\| \frac{d\rho_t}{dt} \right\|_1 \int_0^\infty \frac{du}{(\kappa_{\min}(\rho_t) + u)^2}. \end{aligned} \quad (\text{C3})$$

Finally, by evaluating the integral, one gets

$$\left| \frac{d}{dt} \text{Tr}(\rho_0 \ln \rho_t) \right| \leq \frac{\kappa_{\max}(\rho_0)}{\kappa_{\min}(\rho_t)} \left\| \frac{d\rho_t}{dt} \right\|_1, \quad (\text{C4})$$

which in turn depends on the Schatten speed, thus concluding our proof.

### D. QUANTUM RELATIVE ENTROPY FOR SINGLE-QUBIT STATES

In this Appendix, we derive a general formula for the quantum relative entropy for the single-qubit states  $\rho_1 = (1/2)(\mathbb{I} + \vec{r}_1 \cdot \vec{\sigma})$ , and  $\rho_2 = (1/2)(\mathbb{I} + \vec{r}_2 \cdot \vec{\sigma})$ , where  $\vec{r}_1 = r_1 \hat{r}_1$  and  $\vec{r}_2 = r_2 \hat{r}_2$  are three-dimensional Bloch vectors, with  $\vec{\sigma} = (\sigma_x, \sigma_y, \sigma_z)$  being the vector of Pauli matrices, and  $\mathbb{I}$  is the  $2 \times 2$  identity matrix. By using the integral representation of the logarithm of the density matrix, one gets [see Eq. (A1)]

$$\begin{aligned} S(\rho_1 || \rho_2) &= \text{Tr}[\rho_1 (\ln \rho_1 - \ln \rho_2)] \\ &= \sum_{l=1,2} (-1)^l \int_0^\infty du \text{Tr}[\rho_1 (\rho_l + u\mathbb{I})^{-1}]. \end{aligned} \quad (\text{D1})$$

Next, it can be readily shown that [127]

$$\begin{aligned} (\rho_l + u\mathbb{I})^{-1} &= 2[(1+2u)\mathbb{I} + \vec{r}_l \cdot \vec{\sigma}]^{-1} \\ &= \frac{2[(1+2u)\mathbb{I} - \vec{r}_l \cdot \vec{\sigma}]}{(1+2u)^2 - r_l^2}, \end{aligned} \quad (\text{D2})$$

for all  $l = \{1, 2\}$ . By combining Eqs. (D1) and (D2), we arrive at the result

$$\begin{aligned} S(\rho_1 \|\rho_2) &= 2 \sum_{l=1,2} (-1)^l \left\{ \int_0^\infty du \frac{1+2u}{(1+2u)^2 - r_l^2} \right. \\ &\quad \left. - \text{Tr}[(\vec{r}_l \cdot \vec{\sigma})\rho_1] \int_0^\infty \frac{du}{(1+2u)^2 - r_l^2} \right\}, \end{aligned} \quad (\text{D3})$$

where we have used that  $\text{Tr}(\rho_1) = 1$ . Next, by applying the algebraic identities  $\text{Tr}(\vec{r}_l \cdot \vec{\sigma}) = 0$ ,  $\text{Tr}(\mathbb{I}) = 2$ , and also  $\text{Tr}[(\vec{r}_1 \cdot \vec{\sigma})(\vec{r}_l \cdot \vec{\sigma})] = 2(\vec{r}_1 \cdot \vec{r}_l)$ , we have that Eq. (D3) becomes

$$\begin{aligned} S(\rho_1 \|\rho_2) &= 2 \sum_{l=1,2} (-1)^l \left\{ \int_0^\infty du \frac{1+2u}{(1+2u)^2 - r_l^2} \right. \\ &\quad \left. - (\vec{r}_1 \cdot \vec{r}_l) \int_0^\infty \frac{du}{(1+2u)^2 - r_l^2} \right\}. \end{aligned} \quad (\text{D4})$$

Next, by computing the integrals and proceeding with some algebraic manipulations, it follows that the quantum relative entropy for arbitrary single-qubit states is given by

$$\begin{aligned} S(\rho_1 \|\rho_2) &= \frac{1}{2} \sum_{l=1,2} (-1)^{l+1} \left\{ \ln(1 - r_l^2) \right. \\ &\quad \left. + r_1(\hat{r}_1 \cdot \hat{r}_l) \ln\left(\frac{1+r_l}{1-r_l}\right) \right\}, \end{aligned} \quad (\text{D5})$$

where we have used the following expressions

$$\int_0^\infty \frac{du}{(1+2u)^2 - r_l^2} = \frac{1}{4r_l} \ln\left(\frac{1+r_l}{1-r_l}\right), \quad (\text{D6})$$

and also

$$\int_0^\infty du \frac{1+2u}{(1+2u)^2 - r_l^2} = -\frac{1}{4} \ln(1 - r_l^2). \quad (\text{D7})$$

In detail, note that Eq. (D5) can be also written as

$$\begin{aligned} S(\rho_1 \|\rho_2) &= \frac{1}{2} \ln\left(\frac{1-r_1^2}{1-r_2^2}\right) + \frac{r_1}{2} \left[ \ln\left(\frac{1+r_1}{1-r_1}\right) \right. \\ &\quad \left. - (\hat{r}_1 \cdot \hat{r}_2) \ln\left(\frac{1+r_2}{1-r_2}\right) \right]. \end{aligned} \quad (\text{D8})$$

Based on Eq. (D8), it follows that the quantum relative entropy  $S(\rho_2 \|\rho_1)$  reads as

$$\begin{aligned} S(\rho_2 \|\rho_1) &= -\frac{1}{2} \ln\left(\frac{1-r_1^2}{1-r_2^2}\right) + \frac{r_2}{2} \left[ \ln\left(\frac{1+r_2}{1-r_2}\right) \right. \\ &\quad \left. - (\hat{r}_1 \cdot \hat{r}_2) \ln\left(\frac{1+r_1}{1-r_1}\right) \right]. \end{aligned} \quad (\text{D9})$$

In particular, for two maximally distinguishable single-qubit states with  $\hat{r}_1 \cdot \hat{r}_2 = 0$ , Eqs. (D8) and (D9) become  $S(\rho_{1,2} \|\rho_{2,1}) = (1/2) \ln[(1 - r_{1,2}^2)/(1 - r_{2,1}^2)] + (r_{1,2}/2) \ln[(1 + r_{1,2})/(1 - r_{1,2})]$ .

Importantly, Eqs. (D8) and (D9) clearly show that the quantum relative entropy is asymmetric for arbitrary single-qubit states, i.e.,  $S(\rho_1 \|\rho_2) \neq S(\rho_2 \|\rho_1)$ . However, Eqs. (D8) and (D9) are expected to recover the same result for the particular case where states  $\rho_1$  and  $\rho_2$  are related to each other by a unitary evolution. To see this point, suppose that  $\rho_2 = V\rho_1V^\dagger = (1/2)(\mathbb{I} + \vec{v} \cdot \vec{\sigma})$ , where  $V^\dagger = V^{-1}$  is a unitary matrix, with  $VV^\dagger = V^\dagger V = \mathbb{I}$ . Here,  $\vec{v} = r_1\hat{v}$ , where  $\hat{v}$  is a unit vector. In words, the unitary transformation is expected to rotate the probe state (i.e., by changing the direction of unit vector  $\vec{r}_1$  in the Bloch sphere), but does not change the purity degree of the quantum state. Hence, we have that  $S(\rho_1 \|\rho_2) = S(V\rho_1V^\dagger \|\rho_1) = (r_1/2)(1 - \hat{r}_1 \cdot \hat{v}) \ln[(1 + r_1)/(1 - r_1)]$ .

- 
- [1] V. Vedral, “The role of relative entropy in quantum information theory,” *Rev. Mod. Phys.* **74**, 197 (2002).
- [2] P. J. Coles, M. Berta, M. Tomamichel, and S. Wehner, “Entropic uncertainty relations and their applications,” *Rev. Mod. Phys.* **89**, 015002 (2017).
- [3] P. J. Coles, V. Katariya, S. Lloyd, I. Marvian, and M. M. Wilde, “Entropic Energy-Time Uncertainty Relation,” *Phys. Rev. Lett.* **122**, 100401 (2019).
- [4] G. Vallone, D. G. Marangon, M. Tomasin, and P. Villoresi, “Quantum randomness certified by the uncertainty principle,” *Phys. Rev. A* **90**, 052327 (2014).
- [5] N. J. Cerf, M. Bourennane, A. Karlsson, and N. Gisin, “Security of Quantum Key Distribution Using  $d$ -Level Systems,” *Phys. Rev. Lett.* **88**, 127902 (2002).
- [6] N. Y. Halpern, A. Bartolotta, and J. Pollock, “Entropic uncertainty relations for quantum information scrambling,” *Commun. Phys.* **2**, 92 (2019).
- [7] L. Amico, R. Fazio, A. Osterloh, and V. Vedral, “Entanglement in many-body systems,” *Rev. Mod. Phys.* **80**, 517 (2008).
- [8] S. Das, S. Khatry, G. Siopsis, and M. M. Wilde, “Fundamental limits on quantum dynamics based on entropy change,” *J. Math. Phys.* **59**, 012205 (2018).
- [9] B. Mohan, S. Das, and A. K. Pati, “Quantum speed limits for information and coherence,” *New J. Phys.* **24**, 065003 (2022).

- [10] P. Faist, “Quantum Coarse-Graining: An Information-Theoretic Approach to Thermodynamics,” [arXiv:1607.03104](https://arxiv.org/abs/1607.03104).
- [11] M. Piani, “Relative Entropy of Entanglement and Restricted Measurements,” *Phys. Rev. Lett.* **103**, 160504 (2009).
- [12] A. Streltsov, G. Adesso, and M. B. Plenio, “Colloquium: Quantum coherence as a resource,” *Rev. Mod. Phys.* **89**, 041003 (2017).
- [13] G. Gour, I. Marvian, and R. W. Spekkens, “Measuring the quality of a quantum reference frame: The relative entropy of frameness,” *Phys. Rev. A* **80**, 012307 (2009).
- [14] G. T. Landi and M. Paternostro, “Irreversible entropy production: From classical to quantum,” *Rev. Mod. Phys.* **93**, 035008 (2021).
- [15] N. Megier, A. Smirne, and B. Vacchini, “Entropic Bounds on Information Backflow,” *Phys. Rev. Lett.* **127**, 030401 (2021).
- [16] F. Settimo, H.-P. Breuer, and B. Vacchini, “Entropic and trace-distance-based measures of non-Markovianity,” *Phys. Rev. A* **106**, 042212 (2022).
- [17] E. Petz, “Geometry of canonical correlation on the state space of a quantum system,” *J. Math. Phys.* **35**, 780 (1994).
- [18] H. J. D. Miller, M. Scandi, J. Anders, and M. Perarnau-Llobet, “Work Fluctuations in Slow Processes: Quantum Signatures and Optimal control,” *Phys. Rev. Lett.* **123**, 230603 (2019).
- [19] H. J. D. Miller, G. Guarnieri, Mark T. Mitchison, and J. Goold, “Quantum Fluctuations Hinder Finite-Time Information Erasure near the Landauer Limit,” *Phys. Rev. Lett.* **125**, 160602 (2020).
- [20] S. Floerchinger and T. Haas, “Thermodynamics from relative entropy,” *Phys. Rev. E* **102**, 052117 (2020).
- [21] C. Bény and T. J. Osborne, “Information-geometric approach to the renormalization group,” *Phys. Rev. A* **92**, 022330 (2015).
- [22] A. P. Majtey, P. W. Lamberti, and D. P. Prato, “Jensen-Shannon divergence as a measure of distinguishability between mixed quantum states,” *Phys. Rev. A* **72**, 052310 (2005).
- [23] P. W. Lamberti, A. P. Majtey, A. Borrás, M. Casas, and A. Plastino, “Metric character of the quantum Jensen-Shannon divergence,” *Phys. Rev. A* **77**, 052311 (2008).
- [24] J. Briët and P. Harremoës, “Properties of classical and quantum Jensen-Shannon divergence,” *Phys. Rev. A* **79**, 052311 (2009).
- [25] S. Kullback and R. A. Leibler, “On information and sufficiency,” *Ann. Math. Statist.* **22**, 79 (1951).
- [26] J. Dajka, J. Łuczka, and P. Hänggi, “Distance between quantum states in the presence of initial qubit-environment correlations: A comparative study,” *Phys. Rev. A* **84**, 032120 (2011).
- [27] L. Rossi, A. Torsello, E. R. Hancock, and R. C. Wilson, “Characterizing graph symmetries through quantum Jensen-Shannon divergence,” *Phys. Rev. E* **88**, 032806 (2013).
- [28] W. Roga, M. Fannes, and K. Życzkowski, “Universal Bounds for the Holevo Quantity, Coherent Information, and the Jensen-Shannon Divergence,” *Phys. Rev. Lett.* **105**, 040505 (2010).
- [29] C. Radhakrishnan, M. Parthasarathy, S. Jambulingam, and T. Byrnes, “Distribution of Quantum Coherence in Multipartite Systems,” *Phys. Rev. Lett.* **116**, 150504 (2016).
- [30] P. Tian and Y. Sun, “Quantifying magic resource via quantum Jensen-Shannon divergence,” *J. Phys. A: Math. Theor.* **58**, 015303 (2024).
- [31] D. P. Pires, K. Modi, and L. C. Céleri, “Bounding generalized relative entropies: Nonasymptotic quantum speed limits,” *Phys. Rev. E* **103**, 032105 (2021).
- [32] V. Pandey, D. Shrimali, B. Mohan, S. Das, and A. K. Pati, “Speed limits on correlations in bipartite quantum systems,” *Phys. Rev. A* **107**, 052419 (2023).
- [33] V. Pandey, S. Bhowmick, B. Mohan, Sohail, and U. Sen, “Fundamental speed limits on entanglement dynamics of bipartite quantum systems,” *Phys. Rev. A* **110**, 052420 (2024).
- [34] J. F. de Sousa and D. P. Pires, “Generalized entropic quantum speed limits,” *Phys. Rev. A* **112**, 012203 (2025).
- [35] M. Nielsen and I. L. Chuang, *Quantum Computation and Quantum Information* (Cambridge University Press, Cambridge, 2000).
- [36] M. Ohya and D. Petz, *Quantum Entropy and Its Use* (Springer, Heidelberg, 2004).
- [37] H. Umegaki, “Conditional expectation in an operator algebra. IV. Entropy and information,” *Kodai Math. Sem. Rep.* **14**, 59 (1962).
- [38] G. Lindblad, “Entropy, information and quantum measurements,” *Commun. Math. Phys.* **33**, 305 (1973).
- [39] T. van Erven and P. Harremoës, “Rényi Divergence and Kullback-Leibler Divergence,” *IEEE Trans. Inf. Theory* **60**, 3797 (2014).
- [40] B. Schumacher and M. D. Westmoreland, “Relative entropy in quantum information theory,” [arXiv:quant-ph/0004045](https://arxiv.org/abs/quant-ph/0004045).
- [41] I. Bengtsson and K. Życzkowski, *Geometry of Quantum States: An Introduction to Quantum Entanglement* (Cambridge University Press, Cambridge, 2006).
- [42] K. M. R. Audenaert and J. Eisert, “Continuity bounds on the quantum relative entropy,” *J. Math. Phys.* **46**, 102104 (2005).
- [43] N. Datta, “Min- and Max-Relative Entropies and a New Entanglement Monotone,” *IEEE Trans. Inf. Theory* **55**, 2816 (2009).
- [44] K. Audenaert, “On the asymmetry of the relative entropy,” *J. Math. Phys.* **54**, 073506 (2013).
- [45] H. Jeffreys, “An invariant form for the prior probability in estimation problems,” *Proc. R. Soc. Lond. A. Math. Phys. Sci.* **186**, 453 (1946).
- [46] P. Kafka, F. Östreicher, and I. Vincze, “On powers of  $f$ -divergences defining a distance,” *Stud. Sci. Math. Hung.* **26**, 415 (1991).
- [47] F. Nielsen, “On a Generalization of the Jensen-Shannon Divergence and the Jensen-Shannon Centroid,” *Entropy* **22**, 221 (2020).
- [48] D. Virosztek, “The metric property of the quantum Jensen-Shannon divergence,” *Adv. Math.* **380**, 107595 (2019).
- [49] R. Bhatia, *Matrix Analysis* (Springer, New York, 1997).
- [50] S. Deffner and S. Campbell, “Quantum speed limits: from Heisenberg’s uncertainty principle to optimal quantum control,” *J. Phys. A: Math. Theor.* **50**, 453001 (2017).
- [51] Z. Gong and R. Hamazaki, “Bounds in nonequilibrium

- quantum dynamics,” *Int. J. Mod. Phys. B* **36**, 2230007 (2022).
- [52] T. Caneva, M. Murphy, T. Calarco, R. Fazio, S. Montangero, V. Giovannetti, and G. E. Santoro, “Optimal Control at the Quantum Speed Limit,” *Phys. Rev. Lett.* **103**, 240501 (2009).
- [53] K. Kobayashi and N. Yamamoto, “Quantum speed limit for robust state characterization and engineering,” *Phys. Rev. A* **102**, 042606 (2020).
- [54] B. Mohan and A. K. Pati, “Reverse quantum speed limit: How slowly a quantum battery can discharge,” *Phys. Rev. A* **104**, 042209 (2021).
- [55] J.-Y. Gyhm, D. Rosa, and D. Šafránek, “Minimal time required to charge a quantum system,” *Phys. Rev. A* **109**, 022607 (2024).
- [56] V. Giovannetti, S. Lloyd, and L. Maccone, “The role of entanglement in dynamical evolution,” *EPL* **62**, 615 (2003).
- [57] J. Batle, M. Casas, A. Plastino, and A. R. Plastino, “Connection between entanglement and the speed of quantum evolution,” *Phys. Rev. A* **72**, 032337 (2005).
- [58] J. Batle, M. Casas, A. Plastino, and A. R. Plastino, “Erratum: Connection between entanglement and the speed of quantum evolution [Phys. Rev. A 72, 032337 (2005)],” *Phys. Rev. A* **73**, 049904 (2006).
- [59] F. Centrone and M. Gessner, “Breaking local quantum speed limits with steering,” *Phys. Rev. Res.* **6**, L042067 (2024).
- [60] J. D. Bekenstein, “Energy Cost of Information Transfer,” *Phys. Rev. Lett.* **46**, 623 (1981).
- [61] S. Lloyd, “Ultimate physical limits to computation,” *Nature* **406**, 1047 (2000).
- [62] T. Fogarty, S. Deffner, T. Busch, and S. Campbell, “Orthogonality Catastrophe as a Consequence of the Quantum Speed Limit,” *Phys. Rev. Lett.* **124**, 110601 (2020).
- [63] A. del Campo, “Probing Quantum Speed Limits with Ultracold Gases,” *Phys. Rev. Lett.* **126**, 180603 (2021).
- [64] R. Puebla, S. Deffner, and S. Campbell, “Kibble-Zurek scaling in quantum speed limits for shortcuts to adiabaticity,” *Phys. Rev. Research* **2**, 032020 (2020).
- [65] D. P. Pires and T. R. de Oliveira, “Relative purity, speed of fluctuations, and bounds on equilibration times,” *Phys. Rev. A* **104**, 052223 (2021).
- [66] L. P. García-Pintos, S. B. Nicholson, J. R. Green, A. del Campo, and A. V. Gorshkov, “Unifying Quantum and Classical Speed Limits on Observables,” *Phys. Rev. X* **12**, 011038 (2022).
- [67] D. Tripathy, J. Thingna, and S. Deffner, “Quantum speed limit for the OTOC from an open systems perspective,” [arXiv:2509.13519](https://arxiv.org/abs/2509.13519).
- [68] S. Deffner and E. Lutz, “Generalized Clausius Inequality for Nonequilibrium Quantum Processes,” *Phys. Rev. Lett.* **105**, 170402 (2010).
- [69] E. Aghion and J. R. Green, “Thermodynamic speed limits for mechanical work,” *J. Phys. A: Math. Theor.* **56**, 05LT01 (2023).
- [70] Y. Hasegawa, “Unifying speed limit, thermodynamic uncertainty relation and Heisenberg principle via bulk-boundary correspondence,” *Nat. Commun.* **14**, 2828 (2023).
- [71] F. Impens, F. M. D’Angelis, F. A. Pinheiro, and D. Guéry-Odelin, “Time scaling and quantum speed limit in non-Hermitian Hamiltonians,” *Phys. Rev. A* **104**, 052620 (2021).
- [72] Y.-Y. Wang and M.-F. Fang, “Quantum speed limit time of a non-Hermitian two-level system,” *Chinese Phys. B* **29**, 030304 (2020).
- [73] D. P. Pires, “Unified entropies and quantum speed limits for nonunitary dynamics,” *Phys. Rev. A* **106**, 012403 (2022).
- [74] B. Shanahan, A. Chenu, N. Margolus, and A. del Campo, “Quantum Speed Limits across the Quantum-to-Classical Transition,” *Phys. Rev. Lett.* **120**, 070401 (2018).
- [75] M. Okuyama and M. Ohzeki, “Quantum Speed Limit is Not Quantum,” *Phys. Rev. Lett.* **120**, 070402 (2018).
- [76] R. Hamazaki, “Speed Limits for Macroscopic Transitions,” *PRX Quantum* **3**, 020319 (2022).
- [77] G. Ness, M. R. Lam, W. Alt, D. Meschede, Y. Sagi, and A. Alberti, “Observing crossover between quantum speed limits,” *Sci. Adv.* **7**, 9119 (2021).
- [78] D. V. Villamizar, E. I. Duzzioni, A. C. S. Leal, and R. Auccaise, “Estimating the time evolution of NMR systems via a quantum-speed-limit-like expression,” *Phys. Rev. A* **97**, 052125 (2018).
- [79] D. P. Pires, E. R. deAzevedo, D. O. Soares-Pinto, F. Brito, and J. G. Filgueiras, “Experimental investigation of geometric quantum speed limits in an open quantum system,” *Commun. Phys.* **7**, 142 (2024).
- [80] Y. Wu, J. Yuan, C. Zhang, Z. Zhu, J. Deng, X. Zhang, P. Zhang, Q. Guo, Z. Wang, J. Huang, C. Song, H. Li, D.-W. Wang, H. Wang, and G. S. Agarwal, “Testing the unified bounds of the quantum speed limit,” *Phys. Rev. A* **110**, 042215 (2024).
- [81] Z. Zhu, L. Gao, Z. Bao, L. Xiang, Z. Song, S. Xu, K. Wang, J. Chen, F. Jin, X. Zhu, Y. Gao, Y. Wu, C. Zhang, N. Wang, Y. Zou, Z. Tan, A. Zhang, Z. Cui, F. Shen, J. Zhong, T. Li, J. Deng, X. Zhang, H. Dong, P. Zhang, Z. Wang, C. Song, C. Cheng, Q. Guo, H. Li, H. Wang, H.-Q. Lin, and R. Mondaini, “Observation of minimal and maximal speed limits for few and many-body states,” *Nat. Commun.* **16**, 1255 (2025).
- [82] L. Mandelstam and I. Tamm, “The uncertainty relation between energy and time in non-relativistic quantum mechanics,” in *Selected Papers*, edited by B. M. Bolotovskii, V. Y. Frenkel, and R. Peierls (Springer, Berlin, Heidelberg, 1991) pp. 115–123.
- [83] N. Margolus and L. B. Levitin, “The maximum speed of dynamical evolution,” *Physica D* **120**, 188 (1998).
- [84] L. B. Levitin and T. Toffoli, “Fundamental Limit on the Rate of Quantum Dynamics: The Unified Bound Is Tight,” *Phys. Rev. Lett.* **103**, 160502 (2009).
- [85] D. Mondal, C. Datta, and S. Sazim, “Quantum coherence sets the quantum speed limit for mixed states,” *Phys. Lett. A* **380**, 689 (2016).
- [86] N. Hörnedal, D. Allan, and O. Sönnernborn, “Extensions of the Mandelstam-Tamm quantum speed limit to systems in mixed states,” *New. J. Phys.* **24**, 055004 (2022).
- [87] N. Hörnedal and O. Sönnernborn, “Margolus-Levitin quantum speed limit for an arbitrary fidelity,” *Phys. Rev. Res.* **5**, 043234 (2023).
- [88] V. Giovannetti, S. Lloyd, and L. Maccone, “Quantum limits to dynamical evolution,” *Phys. Rev. A* **67**, 052109 (2003).
- [89] M. Andrecut and M. K. Ali, “The adiabatic analogue of the Margolus-Levitin theorem,” *J. Phys. A: Math. Gen.* **37**, L157 (2004).
- [90] M. Okuyama and M. Ohzeki, “Comment on ‘Energy-

- time uncertainty relation for driven quantum systems’,” *J. Phys. A: Math. Theor.* **51**, 318001 (2018).
- [91] N. Hörnedal and O. Sönnernborn, “Closed systems refuting quantum-speed-limit hypotheses,” *Phys. Rev. A* **108**, 052421 (2023).
- [92] M. Gessner and A. Smerzi, “Statistical speed of quantum states: Generalized quantum Fisher information and Schatten speed,” *Phys. Rev. A* **97**, 022109 (2018).
- [93] H. Wang and X. Qiu, “Generalized Coherent Quantum Speed Limits,” *arXiv:2401.01746*.
- [94] G. Ness, A. Alberti, and Y. Sagi, “Quantum Speed Limit for States with a Bounded Energy Spectrum,” *Phys. Rev. Lett.* **129**, 140403 (2022).
- [95] M. M. Taddei, B. M. Escher, L. Davidovich, and R. L. de Matos Filho, “Quantum Speed Limit for Physical Processes,” *Phys. Rev. Lett.* **110**, 050402 (2013).
- [96] A. del Campo, I. L. Egusquiza, M. B. Plenio, and S. F. Huelga, “Quantum Speed Limits in Open System Dynamics,” *Phys. Rev. Lett.* **110**, 050403 (2013).
- [97] S. Deffner and E. Lutz, “Quantum Speed Limit for Non-Markovian Dynamics,” *Phys. Rev. Lett.* **111**, 010402 (2013).
- [98] Z. Sun, J. Liu, J. Ma, and X. Wang, “Quantum speed limits in open systems: Non-Markovian dynamics without rotating-wave approximation,” *Sci. Rep.* **5**, 8444 (2015).
- [99] X. Meng, C. Wu, and H. Guo, “Minimal evolution time and quantum speed limit of non-Markovian open systems,” *Sci. Rep.* **5**, 16357 (2015).
- [100] N. Mirkin, F. Toscano, and D. A. Wisniacki, “Quantum-speed-limit bounds in an open quantum evolution,” *Phys. Rev. A* **94**, 052125 (2016).
- [101] M. Cianciaruso, S. Maniscalco, and G. Adesso, “Role of non-Markovianity and backflow of information in the speed of quantum evolution,” *Phys. Rev. A* **96**, 012105 (2017).
- [102] J. Teittinen, H. Lyyra, and S. Maniscalco, “There is no general connection between the quantum speed limit and non-Markovianity,” *New J. Phys.* **21**, 123041 (2019).
- [103] J. Teittinen and S. Maniscalco, “Quantum Speed Limit and Divisibility of the Dynamical Map,” *Entropy* **23**, 331 (2021).
- [104] D. P. Pires, M. Cianciaruso, L. C. Céleri, G. Adesso, and D. O. Soares-Pinto, “Generalized Geometric Quantum Speed Limits,” *Phys. Rev. X* **6**, 021031 (2016).
- [105] E. O’Connor, G. Guarneri, and S. Campbell, “Action quantum speed limits,” *Phys. Rev. A* **103**, 022210 (2021).
- [106] K. Lan, S. Xie, and X. Cai, “Geometric quantum speed limits for Markovian dynamics in open quantum systems,” *New J. Phys.* **24**, 055003 (2022).
- [107] B. Russell and S. Stepney, “Applications of Finsler geometry to speed limits to quantum information processing,” *Int. J. Found. Comput. Sci.* **25**, 489 (2014).
- [108] S. Deffner, “Geometric quantum speed limits: a case for Wigner phase space,” *New J. Phys.* **19**, 103018 (2017).
- [109] K. Funo, N. Shiraishi, and K. Saito, “Speed limit for open quantum systems,” *New J. Phys.* **21**, 013006 (2019).
- [110] T. Van Vu and Y. Hasegawa, “Geometrical Bounds of the Irreversibility in Markovian Systems,” *Phys. Rev. Lett.* **126**, 010601 (2021).
- [111] S. Nakajima and Y. Utsumi, “Speed limits of the trace distance for open quantum system,” *New J. Phys.* **24**, 095004 (2022).
- [112] A. J. B. Rosal, D. O. Soares-Pinto, and D. P. Pires, “Quantum speed limits based on Schatten norms: Universality and tightness,” *Phys. Lett. A* **534**, 130250 (2025).
- [113] I. Csiszár, “On information-type measure of difference of probability distributions and indirect observations,” *Stud. Sci. Math. Hung.* **2**, 299 (1967).
- [114] R. Bathia, *Matrix Analysis* (Springer-Verlag, New York, 1997).
- [115] M. Oszmaniec, R. Augusiak, C. Gogolin, J. Kołodyński, A. Acín, and M. Lewenstein, “Random Bosonic States for Robust Quantum Metrology,” *Phys. Rev. X* **6**, 041044 (2016).
- [116] S. Yu, “Quantum Fisher Information as the Convex Roof of Variance,” *arXiv:1302.5311*.
- [117] G. Tóth and D. Petz, “Extremal properties of the variance and the quantum Fisher information,” *Phys. Rev. A* **87**, 032324 (2013).
- [118] G. Tóth, “Lower bounds on the quantum Fisher information based on the variance and various types of entropies,” *arXiv:1701.07461*.
- [119] D. Girolami, “Observable Measure of Quantum Coherence in Finite Dimensional Systems,” *Phys. Rev. Lett.* **113**, 170401 (2014).
- [120] S. Khatri, K. Sharma, and M. M. Wilde, “Information-theoretic aspects of the generalized amplitude-damping channel,” *Phys. Rev. A* **102**, 012401 (2020).
- [121] S.-C. Wang, Z.-W. Yu, W.-J. Zou, and X.-B. Wang, “Protecting quantum states from decoherence of finite temperature using weak measurement,” *Phys. Rev. A* **89**, 022318 (2014).
- [122] T. Van Vu and K. Saito, “Thermodynamic unification of optimal transport: Thermodynamic uncertainty relation, minimum dissipation, and thermodynamic speed limits,” *Phys. Rev. X* **13**, 011013 (2023).
- [123] T. Yada, P.-J. Stas, A. Suleymanzade, E. N. Knall, N. Yoshioka, T. Sagawa, and M. D. Lukin, “Experimentally Probing Entropy Reduction via Iterative Quantum Information Transfer,” *Phys. Rev. X* **15**, 031054 (2025).
- [124] A. Smirne, J. Kołodyński, S. F. Huelga, and R. Demkowicz-Dobrzański, “Ultimate precision limits for noisy frequency estimation,” *Phys. Rev. Lett.* **116**, 120801 (2016).
- [125] D. Toniolo and S. Bose, “Dynamical  $\alpha$ -Rényi Entropies of Local Hamiltonians Grow at Most Linearly in Time,” *Phys. Rev. X* **15**, 031046 (2025).
- [126] M. Suzuki, “Quantum Analysis and Nonequilibrium Response,” *Prog. Theor. Phys.* **100**, 475 (1998).
- [127] D. P. Pires, L. C. Céleri, and D. O. Soares-Pinto, “Geometric lower bound for a quantum coherence measure,” *Phys. Rev. A* **91**, 042330 (2015).